AD-A084 136 CALIFORNIA UNIV SANTA BARBARA F/G 7/4
THE ROLE OF IODINE MOTION ON THE ELECTRONIC PROPERTIES OF TETRA--ETC(U)
MAR 80 S M LATIF N00014-76-C-1044
UNCLASSIFIED NL

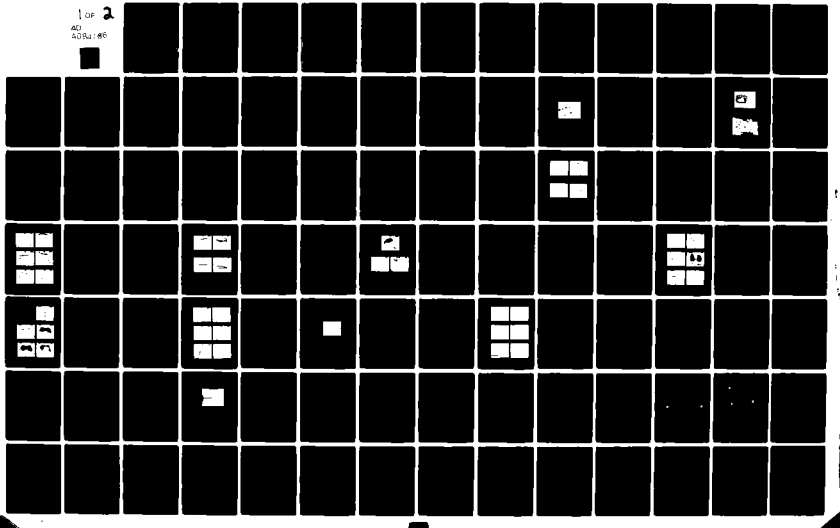

THE ROLE OF IODINE MOTION ON THE ELECTRONIC PROPERTIES OF TETRATHIOFULVALENE IODIDE (TTF-I_n, $n \cong 0.7$)

Technical Report

Shabbir Moiz Latif

March 1980

Office of Naval Research

N00014-76-C-1044

The Regents of the
University of California
Santa Barbara, California 93106

Unclassified

SECURITY CLASSIFICATION OF THIS PAGE (When Data Entered)

REPORT DOCUMENTATION PAGE		READ INSTRUCTIONS BEFORE COMPLETING FORM
1. REPORT NUMBER	2. GOVT ACCESSION NO. AD-A084 136	3. RECIPIENT'S CATALOG NUMBER
4. TITLE (and Subtitle) The Role of Iodine Motion on the Electronic Properties of Tetrathiofulvalene Iodide ($TTF-I_n$ $n \neq 0.7$) Sub Approximately		5. TYPE OF REPORT & PERIOD COVERED Interim Technical Report
		6. PERFORMING ORG. REPORT NUMBER
7. AUTHOR(s) Shabbir Moiz Latif		8. CONTRACT OR GRANT NUMBER(s) N00014-76-C-1044 new
9. PERFORMING ORGANIZATION NAME AND ADDRESS The Regents of the University of California, Santa Barbara, California 93106		10. PROGRAM ELEMENT, PROJECT, TASK AREA & WORK UNIT NUMBERS NR 372-083
11. CONTROLLING OFFICE NAME AND ADDRESS Office of Naval Research Electronics Program Office Arlington, Virginia 22217		12. REPORT DATE Mar[redacted]80
		13. NUMBER OF PAGES
14. MONITORING AGENCY NAME & ADDRESS (If different from Controlling Office)		15. SECURITY CLASS. (of this report) Unclassified
		15a. DECLASSIFICATION/DOWNGRADING SCHEDULE

16. DISTRIBUTION STATEMENT (of this Report)

Approved for public release; distribution unlimited.

17. DISTRIBUTION STATEMENT (of the abstract entered in Block 20, if different from Report)

18. SUPPLEMENTARY NOTES

Ph.D. Thesis of S. M. Latif

19. KEY WORDS (Continue on reverse side if necessary and identify by block number)

Tetrathiofulvalene Iodide
$TTF-I_n$
Quasi-One-Dimensional Conductors
Organic Conductors

20. ABSTRACT (Continue on reverse side if necessary and identify by block number)

The response of electric current in the quasi-one-dimensional conductor $TTF-I_n$ ($n \simeq 0.7$) under high electric fields has been investigated. A large portion of this thesis is comprised of presentation and interpretation of

DD FORM 1 JAN 73 1473 EDITION OF 1 NOV 65 IS OBSOLETE S/N 0102-LF-014-6601

Unclassified

SECURITY CLASSIFICATION OF THIS PAGE (When Data Entered)

10724/52

JCR

some puzzling phenomena observed under high pulsed bias. The phenomena include negative-resistance-like behavior, memory effects, erratic occurrence of oscillations with approximately 70 MHz frequency, and several others. The numerical values associated with all the phenomena except the oscillation frequency fluctuate erratically even when the experiments are repeated on the same sample.

The crystal structure of TTF-I_n consists of two incommensurate sublattices, a rigid TTF sublattice and a seemingly flexible iodine sublattice. Based on such structural properties, it is postulated that the iodine ions have appreciable mobility, restrained only due to pinning at impurities and atomic defects. The structure suggests that, under high field, the iodine sublattice transforms from the ordered phase to a disordered phase. It is further postulated that the changes in sample conductance observed under high field are due to a localization of the carriers along the TTF stacks caused by the phase transition of the iodine sublattice.

TABLE OF CONTENTS

1. INTRODUCTION:

BACKGROUND AND MOTIVATION FOR THIS WORK

The tetrathiofulvalene iodide compound ($TTF\text{-}I_n$ with the composition parameter $n \cong 0.7$) is a member of an increasing group of quasi-one-dimensional conductors. It has been known almost since the discovery of $TTF\text{-}I_n$ that the substance has very abnormal electrical properties,[1,2] such as a huge anisotropy, a "metal"-to-insulator transition, and huge temperature hysteresis effects in its electrical conductivity. These peculiar properties might be consequences of an appreciable mobility of the iodine ions along their quasi-one-dimensional channels in the $TTF\text{-}I_n$ structure. It can be predicted from the unusual crystal structure that the iodine ions should have high mobility. In what follows, the crystal structure and the transport properties are summarized to provide a background before discussing the motivation for our research.

1.1 Structure of $TTF\text{-}I_n$

The compound $TTF\text{-}I_n$ exhibits several phases, each with different values of n. Our research dealt with the ordered monoclinic form of $TTF\text{-}I_n$ ($n \cong 0.7$); it is the phase referred to mostly in this thesis. The structure

of this phase of TTF-I_n has been studied by Daly et al.[3] and by Johnson et al.[4] Some of the structural properties are reviewed in Section 1.1.1. To explain certain experimental results observed in the case of the ordered phase, it is important to consider another monoclinic phase called the "disordered phase".[5] Structural properties of the disordered phase are reviewed in Section 1.1.2. The TTF iodide system is a member of a related class of compounds, the TTF halides, which also includes TTF bromide and TTF chloride. The monoclinic TTF-Br_n has a structure[5,6] that is very similar to that of the monoclinic TTF-I_n. Whenever the structural data for TTF-I_n are not available, we have drawn upon the data published for TTF-Br_n.

1.1.1 Incommensurability of TTF and Iodine Sublattices

In what is called the ordered phase, the structure[3,4,6] consists of segregated, alternate stacks of positively charged TTF molecule ions and negatively charged iodine ions. The stacks run parallel to the longitudinal direction of the needle-shaped crystals. Figure 1.1(a) shows the structure of the TTF molecule and Figure 1.1(b) shows the structure of the crystal, viewed down the stacking axis. As shown by the schematic side

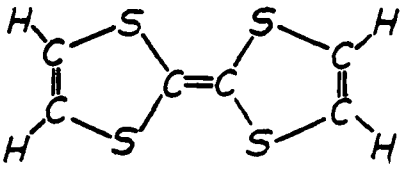

Figure 1.1(a) Tetrathiofulvalene (TTF) Molecule.

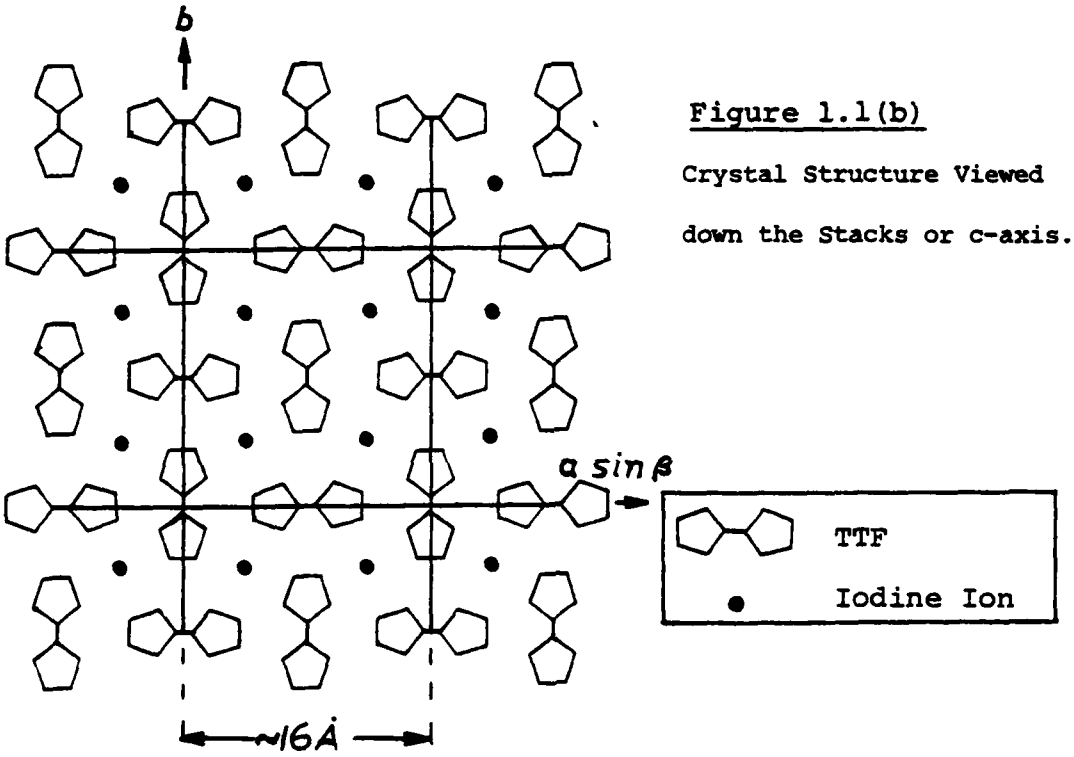

Figure 1.1(b)

Crystal Structure Viewed down the Stacks or c-axis.

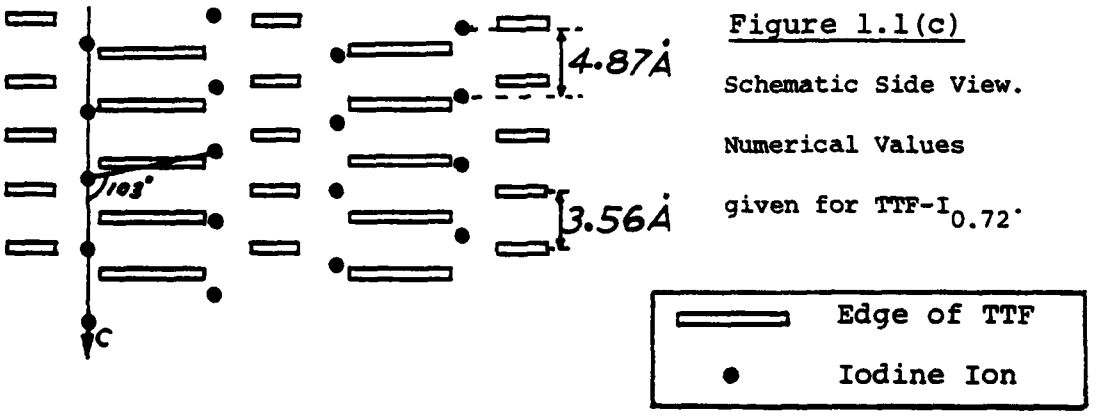

Figure 1.1(c)

Schematic Side View. Numerical Values given for TTF-$I_{0.72}$.

view of the crystal in Figure 1.1(c), both the TTF and the iodine stacks are periodic but their periods are quite unrelated; i.e., the ratio of their periods is not a simple rational number. In fact, the ratio depends on the composition parameter (n), which is not fixed. A series of samples prepared over a range of TTF:halogen ratios by various groups[2,5,6] has shown that the ordered phase is stable over a non-zero range in composition.[7] Specifically, two of the groups[5,6] have demonstrated that the stacking period for bromine ions in TTF-Br_n varies linearly with the composition parameter. Furthermore, each iodine stack [Figure 1.1(c)] is regularly displaced along the stacking axis relative to the adjacent iodine stack such that the iodine ions form a monoclinic sublattice. The tilt angle (β) for this sublattice also depends linearly on the composition parameter n.[5] The TTF molecules form an almost tetragonal sublattice. In other words, the structure consists of two sublattices that are incommensurate with each other in the stacking direction. The stack period and the tilt angle β for the iodine sublattice varies linearly with the composition parameter while the remaining cell parameters of both the sublattice remain constant over the homogeneity range.

Table 1.1 shows the dimensions of the unit cell of both the sublattices for TTF-$I_{0.72}$.

Table 1.1: Unit Cell Data for $TTF\text{-}I_{0.72}$

(after Scott et al. [5])

	Sublattices: TTF	I	Units
a	15.988	8.19	[Å]
b	16.114	16.11	[Å]
c	3.558	4.87	[Å]
β	90.96	102.82	[Degrees]

There is one stack of iodine ions per stack of TTF molecule ions; thus the ratio of the TTF stack period to the iodine stack period can be used as a direct measure of the composition parameter n with a minor discrepancy.[5,6]

$$n \cong c_{TTF}/c_I$$

This means that, with n ranging from 0.71 to 0.77, the ordered structure could be stable with an iodine stack period, from 4.6 to 5.0 Å, while the period along the TTF stack stays fixed at 3.56 Å ($c_I \cong c_{TTF}/n$). Such structures with a non-zero range in composition are known as "infinitely adaptive structures."[4]

Iodine has a very high electron affinity, and iodine ions in the compound are always singly negatively charged. Thus, one electron per iodine ion is transferred from the TTF stacks to the iodine stack. This means, in this ordered phase of TTF iodide, the hole concentration in the TTF stacks must be equal to the concentration of iodine ions.

1.1.2 Disordered Phase

Different phases of the TTF halides have been reported by Scott et al.[5] and by Samoano et al.[2] Each TTF halide also exhibits a stable disordered phase, with a value $n < 0.7$, in addition to the ordered-phases ($0.7 < n < 0.8$). Scott et al.[5] have discovered that the major characteristic of the disordered phase is the complete disappearance of the halide sublattice x-ray reflections. It seems as if, at low halogen concentrations, the halide sublattice becomes unstable and the halogen forms a "gas" with random positions within their channels, while the TTF sublattice essentially stays the same.[5] In the case of TTF iodide, such a stable disordered-phase is found with $n = 0.69$.[2,5]

1.2 Transport Properties

The electronic conductivity of TTF-I_n ($n \cong 0.7$) in the longitudinal direction is 200 to 500 $(\Omega cm)^{-1}$, while in the transverse direction the conductivity is three to five orders of magnitude less.[1,2] The electronic current in the longitudinal direction is due to hole flow along the TTF stacks.[1,2] The electrons are localized on the iodine ions and do not contribute to the electronic current.

There are four TTF molecules in a subcell of approximate dimension 16Å × 16Å × 3.6Å. For n = 0.7, there are 0.7 holes per TTF molecule. Thus, the carrier concentration should be about 3×10^{21} cm^{-3}. The material can be considered as a degenerately doped p-type semiconductor.

Warmack et al.[1] and Samoano et al.[2] have reported a huge hysteresis in the longitudinal electronic conductivity, during temperature cycling below room temperature. Figure 1.2 shows an example reported by Samoano et al.[2] In general, as the temperature is lowered below 290 K, a transition to a low-conductivity state occurs, and upon warming the material the conductivity rises with a huge hysteresis effect. The cause of such anomalous behavior is not established yet. Samoano et al.[2] suggests this behavior is due to intrachain interaction and

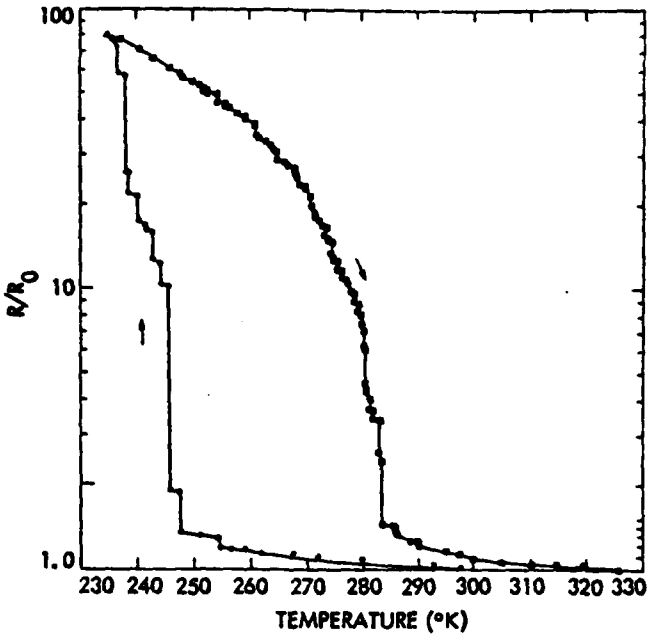

Figure 1.2 Temperature Dependence of the Normalized Resistance of a TTF-$I_{0.71}$ Sample (after Samoano et al. [2]).

associates the series of jumps during the transition with "...portions or domains of the crystal going through the transitions separately." He also reports that "On a few occasions the conductivity did not return to its previous room temperature value upon thermal cycling, returning, for example, to only half its previous value. Previous room temperature conductivities can usually be regained by waiting several hours at room temperature or by heating slightly above room temperature." Also, Warmack et al. have reported that below the transition temperature, the decrease in conductivity continued even if the temperature was held constant (to within ±0.2 K), suggesting that some changes within the sample took place.[1] Transition temperature, size and shape of the hysteresis were found different upon repeated cycling on the same sample. This lack of repetition is also a strong evidence that actual changes took place within the sample during temperature cycling.[1]

1.3 Postulate: A High Iodine Mobility, Limited by Impurities and Defects

It is apparent from the structural data that the TTF molecules form a rigid "backbone" of the crystal and that the iodine ions are confined to channels between the TTF

columns. However, the longitudinal interaction between the TTF molecules and the iodine ions is too weak to lock the latter into a fixed position relative to the TTF sublattice. In the case of TTF-Br_n, Theodorou[8] has evaluated the periodic potential experienced by the bromide sublattice due to the presence of the TTF sublattice and found it to be small. The lattice-period component had a negligible amplitude and the 2nd space-harmonic an amplitude of only $\cong$ 0.14 meV, for $n \cong 0.787$. The Coulomb repulsion between the iodine ions themselves seems to be the dominant force in formation of the iodine sublattice. Specifically, it is responsible both for the periodicity along the iodine stacks, and the interchain correlation that leads to the monoclinic tilt in the iodine sublattice. The iodine ions do not escape from the crystal because the attraction between the positively charged TTF stack and the negatively charged iodine stack lowers the crystal energy. Scott et al.[5] and Torrance and Silverman[9] have calculated Madelung energies of the TTF bromide as functions of the halogen stoichiometry; they showed the actually observed n-ranges are located right at the values for the calculated minima. Finally, there should not be a hard-core interaction between the iodine ions because the distance between iodine ions (4.6-5.0 Å) is appreciably larger than the ionic diameter (4.32 Å).[10]

Under these circumstances the iodine ions should have a high mobility along the smooth array of channels formed by the TTF sublattice. In real crystals, this high ionic mobility along the stacking direction will be limited by pinning at impurities and structural defects, similar to the pinning of dislocations and magnetic domain walls.

The strong hysteresis effect, possibly due to intra-chain interactions, and the evidence of changes within the crystal, (Section 1.2), strongly support the postulate that the iodine ions are mobile within the channels formed by the TTF columns. The conductivity transition could be due to ion motion caused by the thermal stress during temperature cycling. The exact connection between the ion motion and the electronic conductivity during the experiment is not clear. The variable stoichiometry of the compound indicates that it should be possible for iodine chains to compress or expand further within their channels under external force. As discussed in Section 1.1.1, the hole concentration in the TTF stacks should vary directly with the iodine concentration. This change in the iodine concentration would not be more than 10 percent because the spacing between the iodine ions has to be greater than the ionic diameter, 4.6 Å. However, even a small change in carrier concentration could cause

a large change in conductivity if, for example, there is an energy gap close to the Fermi level. It is also conceivable that minor modulation of iodine concentration might cause significant changes in the hole mobility.

X-ray studies at low temperature by Warmack et al.[2] have not revealed any change in the overall structure. However, such studies would only show significant changes in the periodic part of the structure and localized changes in the structure might not be disclosed.

One possible way to study the anomalous behavior of the electronic conductivity seems to be by moving the ions purposely, say by applying an electric field. The questions one might ask are: (a) Can the conductivity transition be modulated by applying electric fields? (b) Can the role of ion motion on the electronic properties of the crystal be studied under applied fields? The search for answers to the above questions motivated us to study this material under high electric fields.

1.4 Outline of this Thesis

A large portion of this thesis comprises of presentation and interpretation of some of the bewildering phenomena observed under high pulsed bias. The phenomena includes negative-resistance-like behavior, memory ef-

fects, and the erratic occurrence of oscillations. In Section 3, the experiments are described in detail and a cross-section of the results is presented to highlight the various phenomena.

A model is presented in Section 4. It is speculated that the abnormal behavior of the electronic conductivity is due to an electrically driven phase transition of the iodine sublattice. This speculation is based on the crystal structure, which suggests that under high field the iodine sublattice transforms from the ordered phase to a disordered phase. This disordered phase is postulated to be slightly unstable and the crystal returns to its original form after a period of a few seconds to a few days.

A summary and some conclusions are presented in Section 5. The electrically driven phase transition, whereby only one of the sublattice is affected, seems to be a fascinating phenomenon. A direct verification of this phenomenon requires much more sophisticated experimental techniques than just the study of current under high pulsed bias. However, such experiments must be preceded by further developments in the preparatory techniques to improve the quality of the crystals. This last section is concluded by presenting several ideas for future research projects.

The above mentioned details, which form the core of this thesis and which are presented in Sections 3 through 5, are preceded by some preliminaries. Measurements of DC conductivity versus temperature similar to that reported by Warmack et al.[1] and by Samoano et al.[2] were performed on a few of the samples available for this project. Results for two of the samples are presented in Section 2. The origin of the samples and the electrical contact techniques are also included in that section.

2. THE SAMPLES: ORIGIN, ELECTRICAL CONTACTS, AND CHARACTERIZATION

2.1 Origin of the Samples

The samples of TTF-I_n(n ~0.7) were kindly supplied by Dr. W. Kaska and Mr. A. Wolff of the Chemistry Department, University of California, Santa Barbara, and by Dr. R.J. Warmack of the Oak Ridge National Laboratory (ORNL). In addition, a few TTF-Br_n samples were provided by Dr. B.A. Scott of the IBM Thomas J. Watson Research Center and, again, by Dr. Kaska and Mr. Wolff.

Most of the samples used for our experiments were those obtained from the UCSB Chemistry Department, but the same effects were observed in the samples from ORNL. Only two TTF-Br_n samples (one from each source) were investigated under high pulsed field. Effects similar to those observed in TTF-I_n were observed in TTF-Br_n, and there do not seem to be any reasons to present them or discuss them separately.

The various TTF-I_n crystals were typically of needle shape with lengths varying from below 0.5 mm to about 5 mm and the cross sectional areas varying from below 0.25×10^{-2} mm^2 to about 1×10^{-2} mm^2. Three samples are shown in Figure 2.1; two of them are with evaporated gold

Figure 2.1 TTF-I_n ($n \cong 0.7$) Crystals.

Three needle shape samples are shown. The bright strips on two of them are evaporated gold contacts. Larger samples had poorer morphological quality. The TTF-Br_n crystals looked similar to the TTF-I_n samples.

stripe contacts. Larger samples had poorer morphological quality than smaller ones. Long samples had twinning and other irregularities, and many of the thicker samples were actually found to be hollow. Thus, most of the time, restricted by the morphological quality, samples of length less than 2 mm were used.

2.2 Electrical Contact Techniques

The crystals were mounted on commercial "flatpacks" (intended for mounting integrated circuit chips), using 1 mil gold wires for contacts [Figure 2.2(a) to (c)]. The ends of the wires were bonded on the flatpack using a thermo-compression bonder. Each wire was connected either to the side or to an end of the crystal. Several different techniques were used to make an ohmic contact between the gold wire and the crystal: (a) the wire was bonded on the crystal using colloidal graphite;[11] (b) gold strips were evaporated on the crystal and the gold wire was bonded on the evaporated gold with either colloidal graphite or silver paint;[12] (c) in a few cases, mechanical contacts were made by just stretching the gold wire over the bare crystal or over the evaporated gold strips.

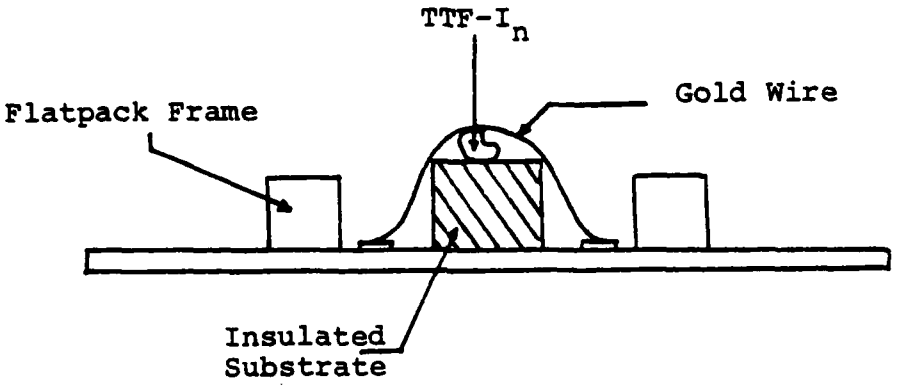

Figure 2.2(a) Schematic Side View of a Sample Mounted on a Commercial Flatpack.

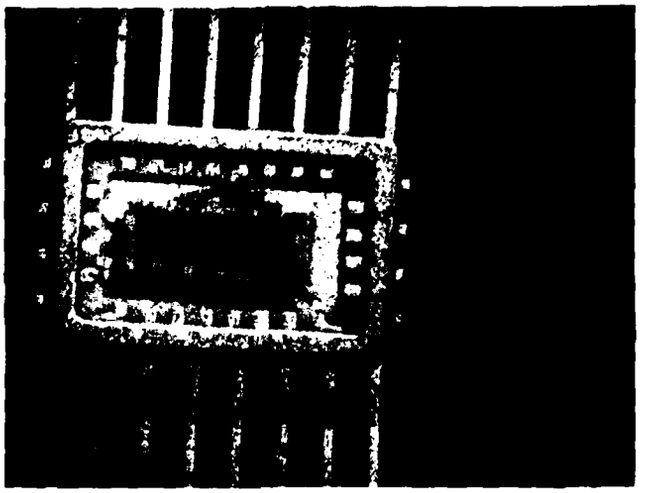

Figure 2.2(b) Top View of a Crystal Mounted on a Flatpack.

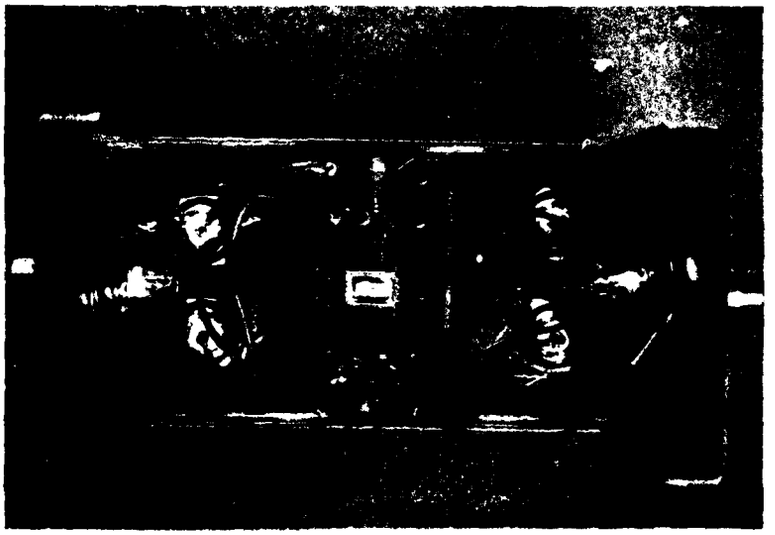

Figure 2.2(c) Top View of the Mounting Set-up.

Enough slack was kept on the gold wires so that the sample would not be strained. For mechanical contacts, the wire was stretched as lightly as possible to minimize the strain on the sample.

2.3 Characterization: DC Conductivity versus Temperature

It has been reported by Warmack et al.[1] and by Samoano et al.[2] that the dc conductivity of TTF-I_n ($n \cong 0.7$) drops sharply by two to five orders of magnitude as the sample is cooled. They have reported the transition temperature to be between 290 K to 240 K. Upon warming the sample back to room temperature a pronounced hysteresis was observed. One such curve, reported by Samoano et al., has been shown in Section 1. The same experiment was performed by us for characterization of representative samples used in this research project.

The samples were mounted as discussed in Section 2.2 with particular attention to minimize strains on the samples at low temperatures. Four contacts were made and a technique similar to the standard four-point probe method was used. The circuit is shown in Figure 2.3.1. The dc conductance (G_T) was measured by passing a small dc current between contacts #1 and #4 using a constant current source. The potential drop V_{23} was measured

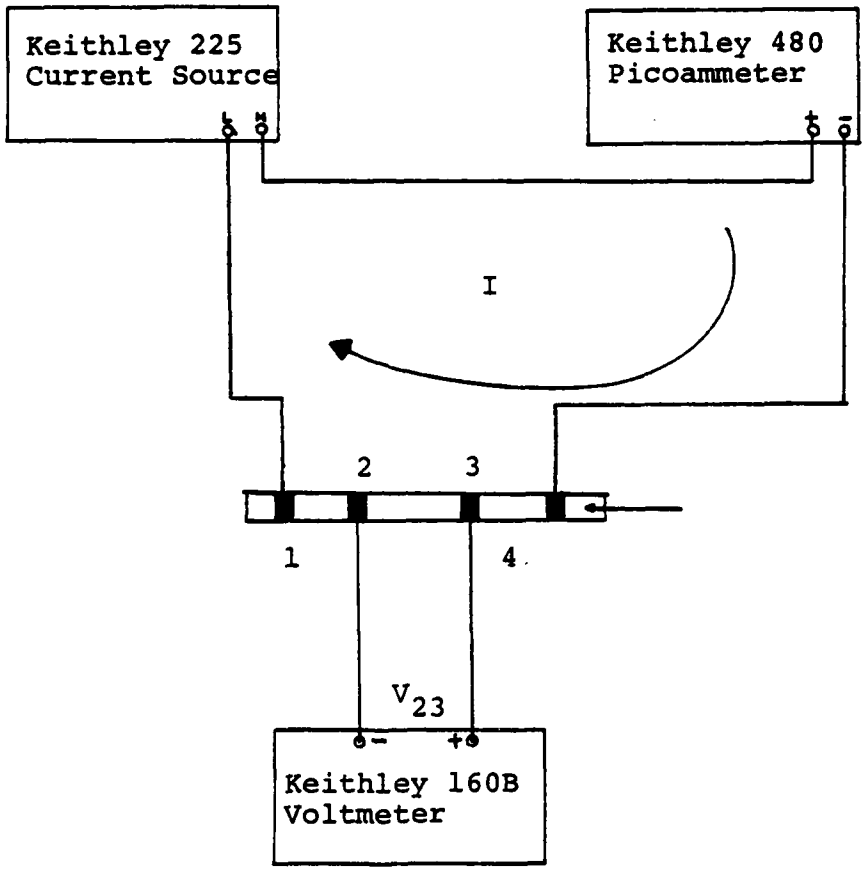

Figure 2.3.1 Circuit used to Measure Bulk DC Conductance

between the two inner contacts using a high-input-impedance voltmeter. Either a Heli-tran® System[13] or a Statham® Test Chamber[14] was used to cool the sample. The temperature was varied manually at the rate of 1 to 3 K per minute and the potential drop was continuously monitored on a strip-chart recorder connected to the voltmeter, while the current was held constant. The power dissipation was kept below 1 μW. The linearity of the current-voltage relationship was also checked at random temperatures during the cycle.

Results for two of the samples are shown in Figure 2.3.2. The results are similar to that reported in the past by other groups.[1,2] In some samples the transitions occurred in small sharp jumps, as reported by Samoano et al.;[2] in others the changes were continuous. Further, as already reported by Warmack et al.[1] and Samoano et al.,[2] in some samples, once below the transition temperature, the conductivity continued to change even if the temperature was held constant. Finally, the data were irreproducible not only from sample to sample but even upon repeating the cycling on the same sample. The transition temperature varied roughly from 290 K to 200 K but for a few samples the change in conductivity was less than an order of magnitude upon cooling to as low as 85 K.

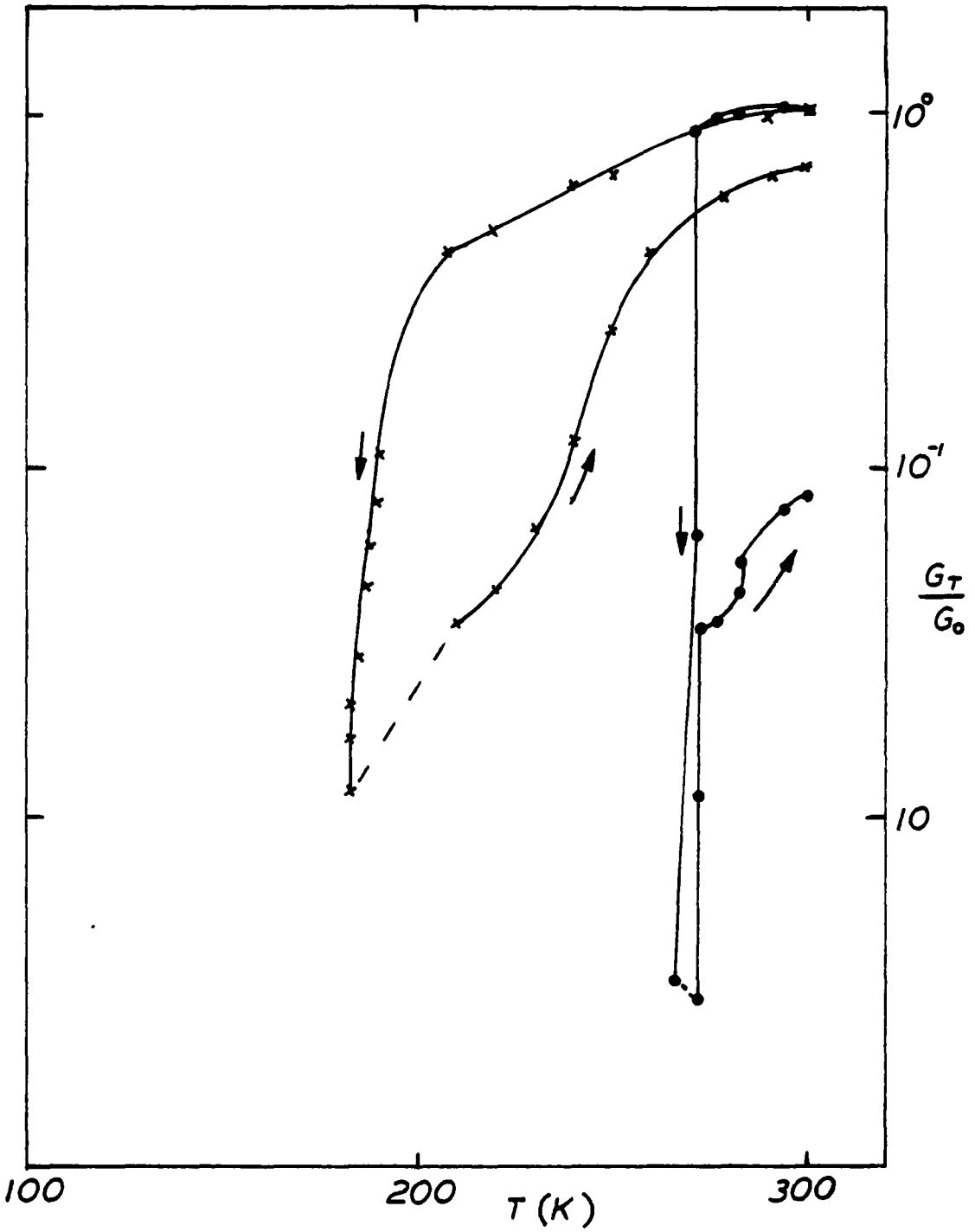

Figure 2.3.2 DC Conductance (G_T) Normalized to the Value at 300 K (G_0), versus Temperature (T), for Two Different TTF-I_n Samples.

We have not performed any measurement of dc conductivity versus temperature on TTF-Br_n. It has been reported[1] that the TTF-Br_n also undergoes a transition to some low-conductivity state upon cooling below 180 K; however, upon warming it returns to the original state without any hysteresis effect.

3. VOLTAGE PULSE EXPERIMENTS

3.1 Circuit

Figure 3.1 shows the circuit used for studying the current through the TTF-I_n crystal in response to an applied field. Voltage pulses were applied between two of the contacts on the sample, and the voltage (V_R) across the series resistor (R_I) was monitored on a storage oscilloscope to study the current through the sample. The value of R_I was chosen small enough (usually 1 Ω) so that the IR drop would be small compared with the amplitude of the applied pulse. Narrow pulses were applied, using manual triggering, with long waiting periods between pulses to avoid heating.

The HP214 pulse generator used has a high output impedance, making the amplitude of the pulse strongly depend on the load impedance. Therefore, a complementary emitter follower (CEF) circuit was usually employed to obtain a low-output-impedance, constant-voltage source. The Darlington Pair configuration was used at the output of the CEF circuit to obtain high effective current gain (β). The circuit is designed such that both the input and the output can be safely varied between +28 and -28 volt without breakdown. Only in a few experiments per-

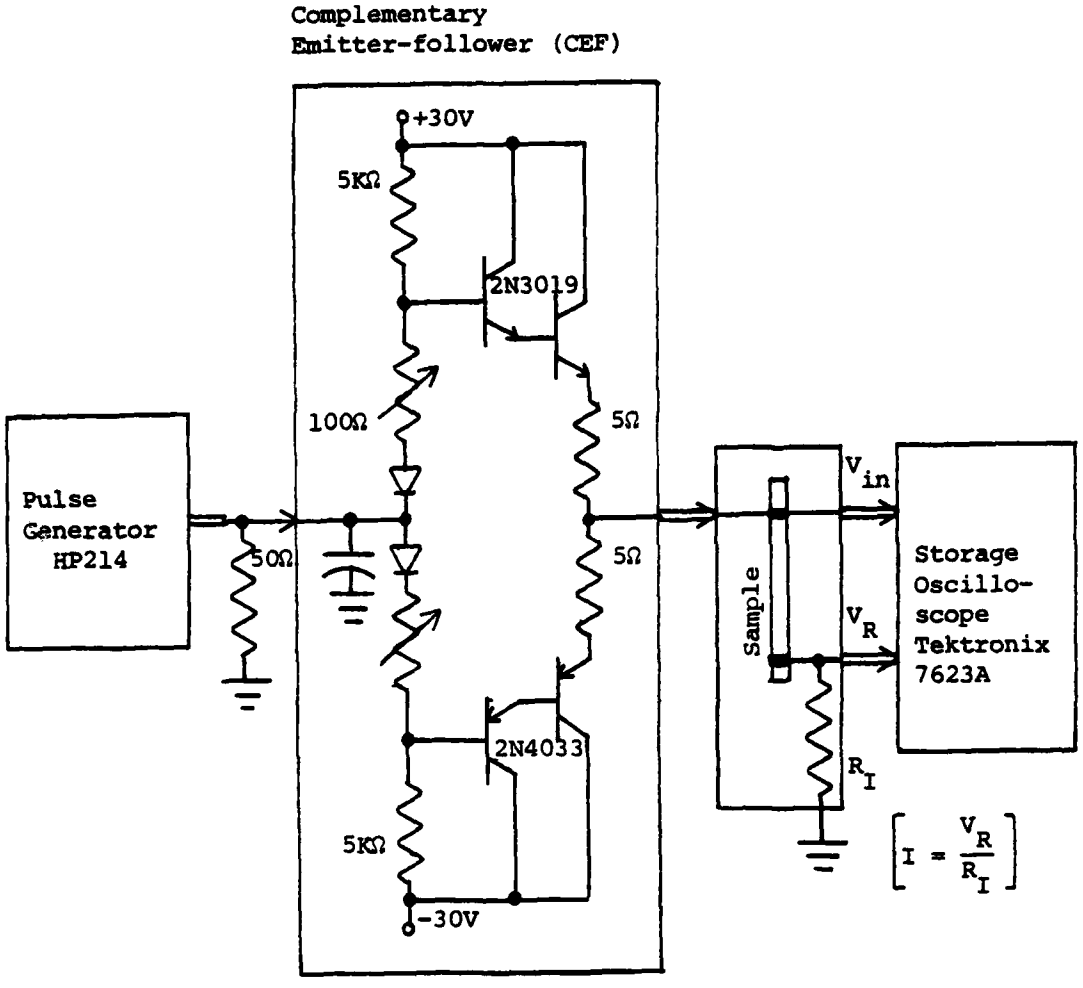

Figure 3.1 Circuit for the Voltage Pulse Experiment.

formed early in the course of this experimentation, was the CEF circuit not used. Such cases will be specifically noted in what follows.

3.2 Results

Several phenomena were observed under applied field:

(a) the current decreases as the voltage is increased above a certain threshold value;

(b) pronounced hysteresis effects appear in the current as the voltage is varied between zero and some value above the threshold;

(c) transition to a metastable "low-conductance state" occurs under high field; the state persists for some time even after the field is removed;

(d) the current decreases as a function of time, while the applied voltage is held constant during a single pulse;

(e) the current sometimes bursts into erratic oscillations with a frequency that is consistently found close to 70 MHz;

(f) the numerical values associated with all the above phenomena except the oscillation frequency fluctuate erractically even when the experiments are repeated on the same sample.

In the rest of this section, we show a cross-section of the experimental results obtained for samples of varying size and morphological quality, varying spacing between contacts, and using various contact techniques described in Section 2.2. All the six phenomena listed above were observed irrespective of these sample parameters. However, because of the quantitative irreproducibility we were not able to study the dependence of the phenomena on the parameters. Thus, the sample parameters are not specified with any of the results reported below.

3.2.1 Negative-Resistance-like Behavior, Hysteresis and Memory Effect

Experimental Procedure: Figures 3.2.1(a) to (d) show the current-voltage characteristics of one single representative sample. They were obtained by applying sequences of voltage pulses[15] with 6.5 μs duration but varying amplitude from zero to some maximum value and back to zero. Each dot in the pictures represents the current (on the vertical axis) in response to a voltage pulse, the amplitude of which is given by the horizontal axis.

Comments: In all four characteristics shown in Figure 3.2.1, the current amplitude increases with an

Figure 3.2.1 Pulsed I-V Characteristics.

I-V characteristics were obtained by applying sequences of voltage pulses of 6.5 μs duration. The amplitude was increased in small steps from zero until the negative-resistance-like behavior appeared and the current dropped to a negligible value; then the amplitude was decreased in small steps back to zero. Hysteresis is apparent. Note that the voltage was zero between pulses, so the difference between pulses with ascending and descending voltage represents a long-term memory effect. All four I-V characteristics were obtained in succession for the same sample and same pair of contacts. Figures (a) and (b) obtained for positive voltage pulses, (c) and (d) for negative voltage pulses.[16]

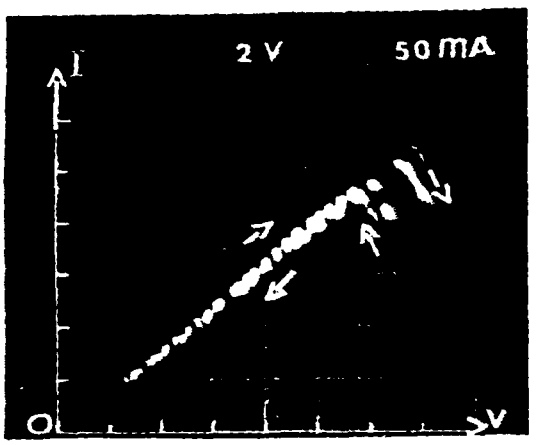

(a)

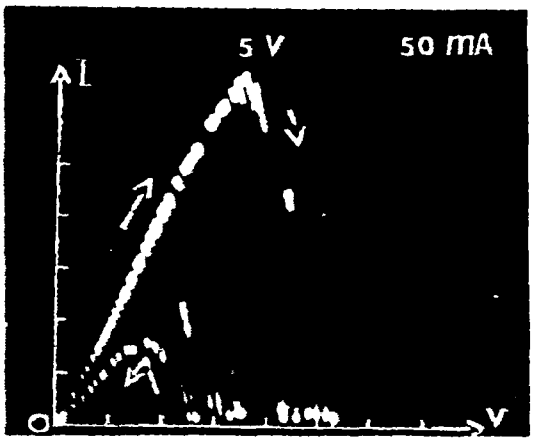

(b)

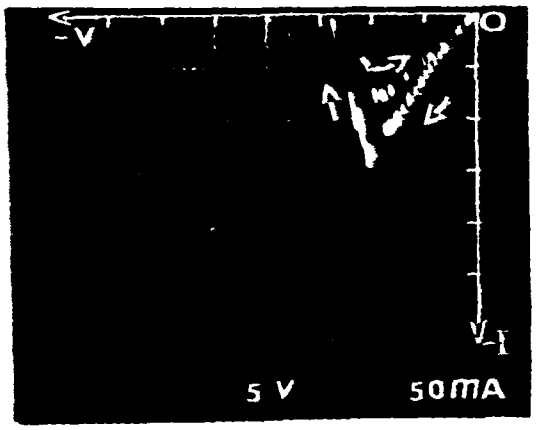

(c)

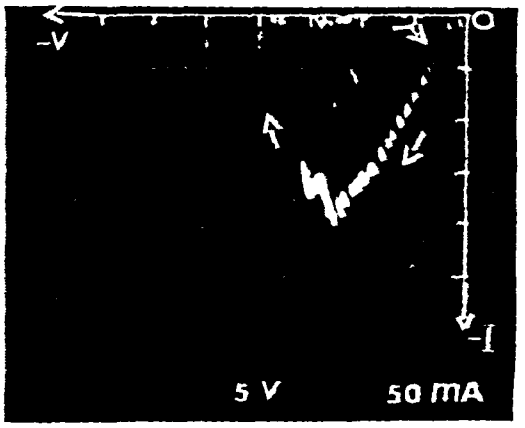

(d)

Figure 3.2.1

increase in voltage amplitudes for small voltages; but above a certain threshold value the current amplitude decreases upon further increase in the amplitude of the voltage pulses.

As the sequence of voltage pulses is continued, but with a decreasing amplitude, the negative-resistance-like behavior is observed again but the current does not retrace the same path as the one followed while the amplitude was increased: a hysteresis effect appears. These effects are much more pronounced in Figure 3.2.1(b) than in (a), (c) or (d).

On account of the manual triggering of the pulse generator, the field is removed between applied pulses for a time interval of at least a few seconds. Evidently, once the transition to the low-conductance state has occurred, the sample stays in that state for some time in the absence of the electric field. There seems to be a strong "memory effect".

As stated, all the results shown were obtained using the same sample. Figures 3.2.1(a) and (b) were obtained in succession using positive voltage pulses and then (c) and (d) were obtained in succession using negative voltage pulses. Poor quantitative reproducibility is evident upon comparing (a) with (b) and (c) with (d).

All the phenomena discussed above were also observed, on the same sample, with pulse duration as low as 300 ns (data not shown). Due to quantitative irreproducibility similar to that observed in Figures 3.2.1(a) to (d), it was impossible to study the variation of the numerical values as a function of pulse duration. However, in general, the voltage amplitude at which the current peaked seemed to be somewhat higher for shorter pulse duration.

Figures 3.2.1(a) to (d) provide a clear picture of the overall current-voltage relationship as the voltage amplitude is varied from pulse to pulse. However, several of the observed phenomena remain obscured by presenting the data in this manner. For example, the streakiness of some of the dots shows that the current changes during a single pulse, but the exact behavior is not at all apparent. Therefore, the phenomena discussed in this section and several additional ones will be highlighted in what follows with various examples recorded in the time domain.

3.2.2 Decrease in Current With Time During a Pulse.

Experimental procedure: Sequences of voltage pulses with varying amplitude but a fixed pulse duration of 600 ns were applied to a single sample. The amplitude was

increased in small steps from 2 V to about 17 V. Selected but typical current waveforms and the corresponding applied pulses of increasing magnitude are shown in Figures 3.2.2(a) to (d). Similarly, Figures 3.2.2(e) and (f) show results while the amplitude is decreased. In Figure 3.2.2(b) two current waveforms are shown because the input at 7.5 V was repeated.

Comments: In Section 3.2.1, it was briefly mentioned that the streakiness in the dots in Figure 3.2.1 is due to changes in current during a single pulse. The pulse response in the time domain elucidates this phenomenon. It is apparent in Figures 3.2.2(d) and (e) that the current decreases as a function of time not only while the voltage is rising for about 200 ns at the start of the pulse but continues to decrease even when the voltage levels. This phenomenon was not seen with amplitudes less than 4 V; above 4 V, it became more prominent with increasing amplitude.

A new phenomenon is revealed by monitoring the current response in the time domain. Above a certain amplitude, the current breaks into oscillations. This behavior, which is apparent in Figure 3.2.2(c), (d) and (e), will be discussed later in Section 3.2.5.

Figure 3.2.2 Decrease in Current with Time During a Pulse.

Current and voltage waveforms as functions of time are shown. Sequences of voltage pulses were applied. The amplitude was varied in steps up to 17 V and was then decreased. Note the decrease in current as a function of time during a single pulse while the voltage is constant. This phenomenon was not present at amplitudes less than 4 volts, but became stronger as the amplitude was increased.

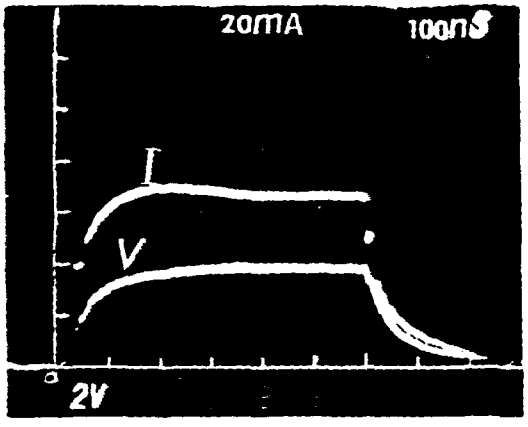

(a)

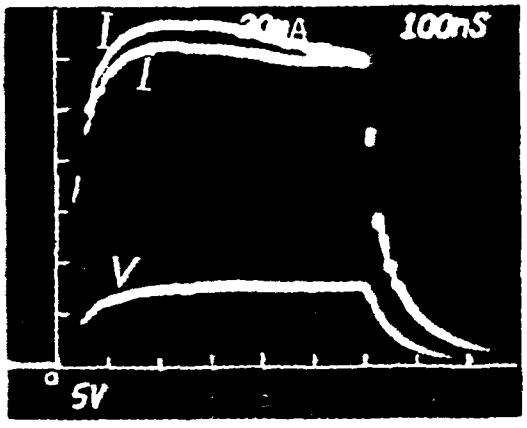

(b)

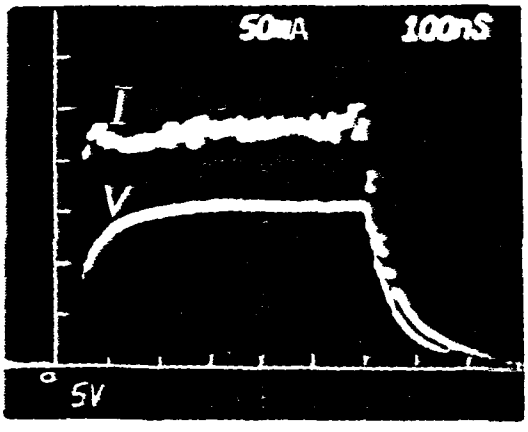

(c)

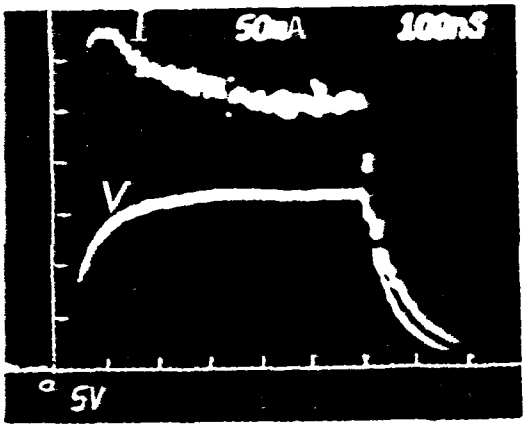

(d)

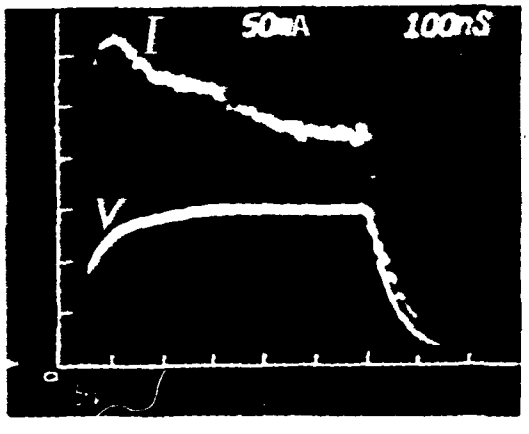

(e)

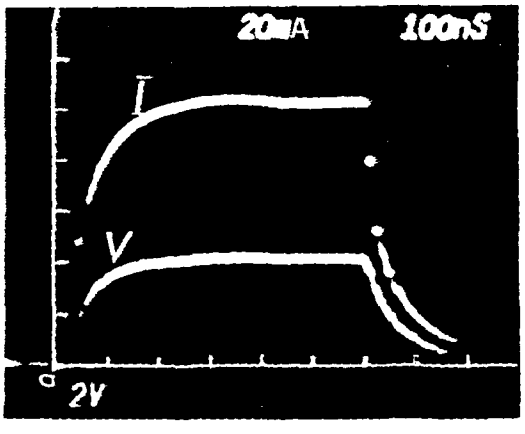

(f)

Figure 3.2.2

3.2.3 Cumulative Transition to a Low-Conductance State by Applying Repeated Pulses with Fixed Amplitude and Duration

Experimental Procedure: The experiment was begun by applying sequences of pulses of 600 ns duration with an amplitude that was increased in steps from 4 V to 27 V. After measuring the response at 27 V amplitude and 600 ns duration, additional pulses were applied with a fixed amplitude of 27 V while increasing the duration in small steps. Pulses were repeated several times at each value. Upon repeated application of pulses of 27 V amplitude and 4 μs pulse duration, a transition to a low-conductance state was observed. The cumulative changes in current from pulse to pulse are shown in Figure 3.2.3(a) to (d). The sequence number is shown next to each waveform.

Comments: As this example shows, the transition occurs just by repeated pulsing with fixed amplitude and duration. To obtain the transition to the low-conductance state, it was not necessary to increase the amplitude of voltage pulses further above a certain threshold value. The manner in which the transition occurred varied not only from sample to sample, but even upon repeated experimentation on the same sample, with all external parameters kept fixed.

Figure 3.2.3 Cumulative Transition to a Low-Conductance State by Applying Repeated Pulses with Fixed Amplitude and Duration.

One or more current waveforms as a function of time are shown in each figure. Upon repeated application of pulses of 27 V amplitude and 4 μs duration, the current amplitude dropped, from pulse to pulse, from over 70 mA to less than 10 mA. Sequence numbers are shown next to each current waveform. The decrease in current as a function of time with constant voltage during a single pulse, and oscillations, are also apparent.

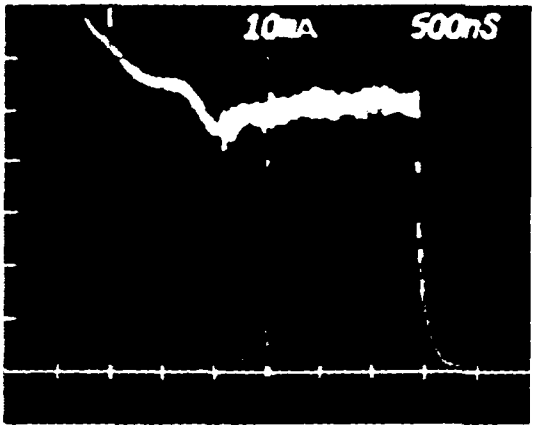

(a)

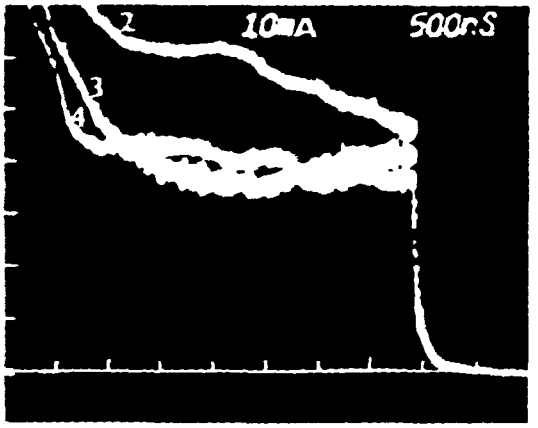

(b)

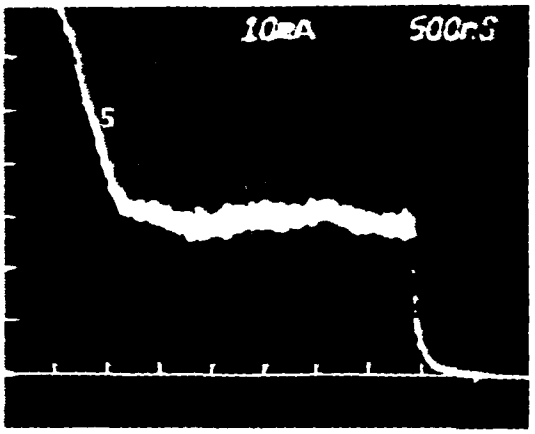

(c)

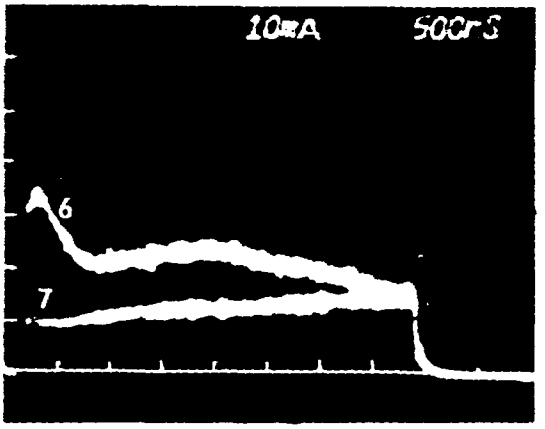

(d)

Figure 3.2.3

Moreover, the results show that the effects on the sample conductance depend not only on the value of the applied field, but also on the length of time that the field is applied. The foregoing conclusion follows from the observation that the transition to the low-conductance state, and the decrease in current as a function of time during a single pulse, were not observed when pulses of 27 V amplitude and 600 ns duration were applied, but they were observed after the pulse duration was increased to 4 μs.

Most of the time, the low-conductance state was found to be reversible. The reversibility aspect is discussed next.

3.2.4 Reversibility of the Transition from High to Low Conductance upon Application of Voltage Pulses of Opposite Polarity

Experimental procedure: The experiment was begun by applying a sequence of 600 ns voltage pulses with increasing amplitude up to 28 V. The sample conductance dropped upon applying repeated pulses of 28 V amplitude. The change in the current amplitude from pulse to pulse is shown in Figure 3.2.4(a). The following sequences of pulses of the same duration were then applied with decreasing amplitude to zero. Unlike the examples in Figure

Figure 3.2.4 Reversibility of the Transition to the Low-Conductance State by Application of Pulses of Opposite Polarity

Current waveforms as a function of time showing that the low-conductance state is reversible by applying pulses of opposite polarity. (a) shows a cumulative decrease in the current amplitude from pulse to pulse, due to repeated application of square voltage pulses of 28 V amplitude and 600 ns duration. (b) and (c) show cumulative increase in current amplitude due to repeated applications of negative pulses with 28 V amplitude and about 1 μs duration.

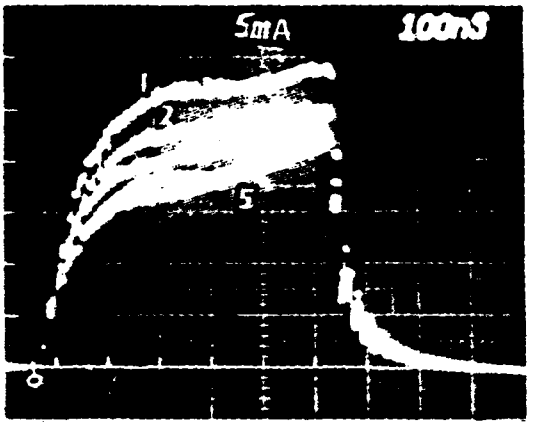

(a)

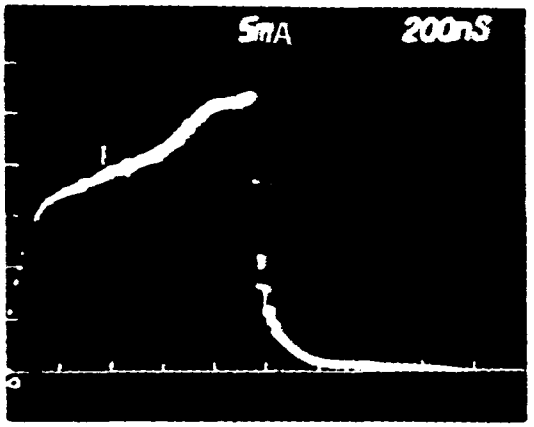

(b)

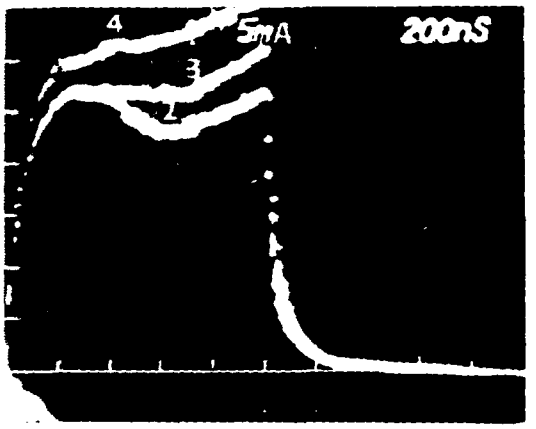

(c)

Figure 3.2.4

3.2.1, the conductance did not increase again by applying pulses with decreasing voltage amplitude. Initially, the current amplitude at 4 V was 2 mA; after the above sequence the current at 4 V was less than 1 mA. Thus, the resistance of the sample more than doubled. The polarity of the pulse generator was now switched to apply pulses of opposite polarity. Again a sequence of voltage pulses of 600 ns width were applied with increasing amplitude up to 28 V. There was no significant change in conductance, so an additional sequence of 28 V pulses was applied. The duration of the pulses was increased in small steps and each pulse was repeated several times. Upon repeated pulsing with 28 V amplitude and 1000 ns duration, the conductance increased. Figure 3.2.4(b) and (c) show the changes from pulse to pulse in the current waveform. Finally, the sequence was completed after applying pulses with decreasing amplitude in small steps. The current at 4 V is then found to be 2 mA which is the same as the initial value observed before the transition to the low-conductance state.

Comments: In Section 3.2.1 (Figure 3.2.1), it was shown that sample conductance decreased with increasing voltage pulse amplitude and the low-conductance state developed. It was also shown that the transition to the low-conductance state was reversible just by applying

pulses of smaller amplitudes. In the present case the transition to the low-conductance state was not reversible just by applying voltage pulses of smaller amplitude but required pulses of opposite polarity (negative voltage pulses). Even though the pulse duration in Figure 3.2.1 is much higher than that in Figure 3.2.4(a), this difference has nothing to do with the different behavior observed in the two samples. As mentioned in Section 3.2.1, phenomena similar to those shown in Figure 3.2.1 were also observed with pulse duration as low as 300 ns. Thus, for reasons unknown, the two samples just behaved differently.

In a few samples, the transition to the low-conductance state was reversed just by aging; i.e., by leaving the sample alone for some time (a few minutes to a few days).

3.2.5 Erratic Oscillations with Approximately 70 MHz Frequency

Experimental procedure: Similar to the previous examples, sequences of voltage pulses of about 400 ns duration were applied. The amplitude was increased in small steps from 2 V up to 15 V and then decreased. The response at each amplitude was checked more than once for reproducibility. Current waveforms at selected inputs

are shown in Figure 3.2.5 (a) to (f). Each of the photographs shows the applied input pulse, and superimposed are one or more current responses.

Comments: The oscillations are obvious in Figure 3.2.5(c) and (d). Note the erratic manner in which the current breaks into oscillation and then decays several times during a single pulse, while the voltage is constant. The frequency of oscillations appears to be about 70 MHz. This frequency was the only quantity in all our experiments that seemed to be reproducible even from sample to sample. The frequency was read from the current waveform on the oscilloscope. Due to the erratic occurrence of the oscillations, no other accurate frequency-measurement technique was attempted.

In Figure 3.2.5(c), (d) and (e), the number next to each waveform shows the order in which they were obtained; no such sequence numbers are shown in Figure 3.2.5(b) because the current amplitude from pulse to pulse changed randomly.

In this example, too, the transition to the low-conductance state is observed. Upon repeated application of 15 V pulses the conductance dropped approximately from $10\times10^{-3}\ \Omega^{-1}$ in Figure 3.2.5(c) to $1.6\times10^{-3}\ \Omega^{-1}$ in Figure

Figure 3.2.5 Erratic Oscillations with Approximately 70 MHz Frequency

Each figure shows one or more current waveforms and the applied input voltage pulse as a function of time. Note the erratic occurrence of oscillations in the current-response at high voltage amplitudes. It is apparent from Figures (c) and (d) that the oscillations are "turned on and off" several times while the voltage is held constant during a single pulse.

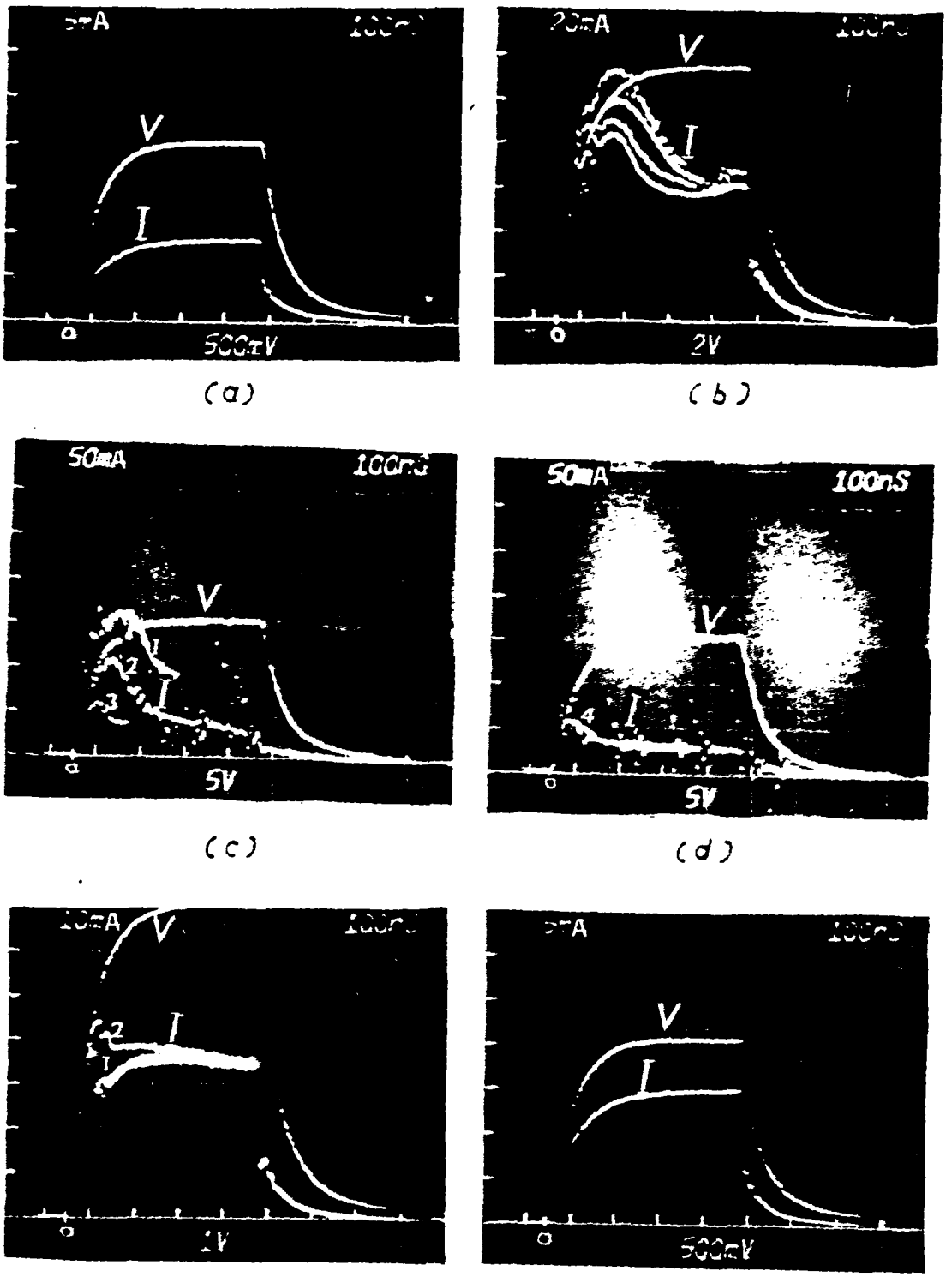
V
I
0
500mV
(a)
20mA
V
I
0
2V
(b)
50mA
100nS
V
I
1
2
3
0
5V
(c)
50mA
100nS
V
I
4
0
5V
(d)
10mA
V
I
2
1
0
2V
(e)
5mA
V
I
0
500mV
(f)

Figure 3.2.5

3.2.5(d). The sample recovered from this state by applying pulses with smaller amplitude. Note that the conductance at 7 V is 5×10^{-3} Ω^{-1} in Figure 3.2.5(e) and at 2 V is 7.5×10^{-3} Ω^{-1} in Figure 3.2.5(f), which is even higher than the value of 4.5×10^{-3} Ω^{-1} in Figure 3.2.5(a).

3.2.6 Pulse Response using "Three-Contact Technique"

Experimental procedure: As in the preceding example, and using the same crystal sample, sequences of voltage pulses were applied with varying amplitude and fixed duration. However, unlike the previous example, in which the voltage pulses were applied between two contacts, in the present case the input pulses were applied simultaneously to two outer contacts with respect to a third, inner contact as shown in Figure 3.2.6(a). Voltage pulses were applied using the outer two contacts as the positive electrodes and the inner contact as a negative electrode. No pulse experiment has been performed with the opposite polarity for this "three-contact technique."

Selected responses for the three-contact technique are shown in Figure 3.2.6(b) to (f). Figures (b) and (c) show the current response for inputs of 3.5 V and 4.5 V, respectively; and Figures (c) through (e) show current waveforms upon repeated pulsing with amplitude of 5 V.

Figure 3.2.6 Pulse Response using "Three-Contact Technique."

(a) The difference between the normally used two-contact technique and the three-contact technique. (b) and (c) Responses at 3.5 V and 4.5 V. (d) through (f) Several responses at 5 V. Note that in (f) one of the two current waveforms does not show any oscillations. The three-contact technique exhibits much stronger oscillations and the oscillation is initiated at lower input than that for the two-contact technique.

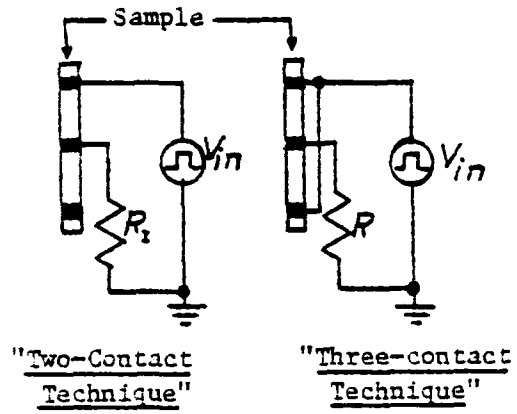

(a)

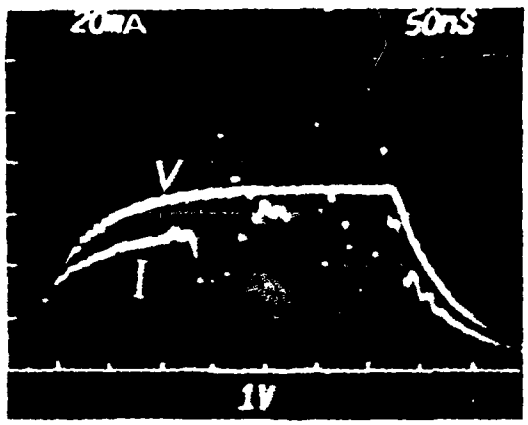

(b)

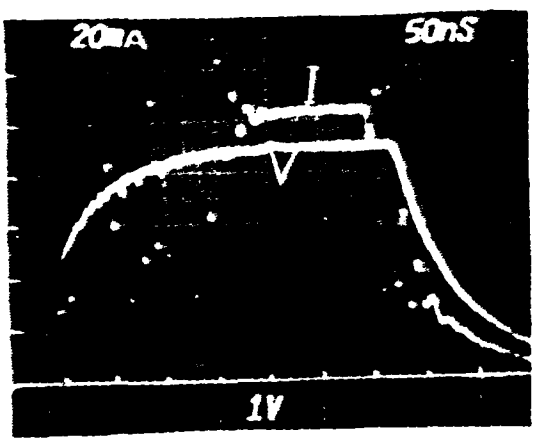

(c)

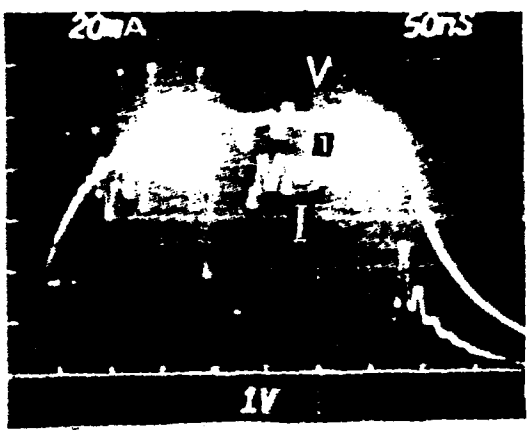

(d)

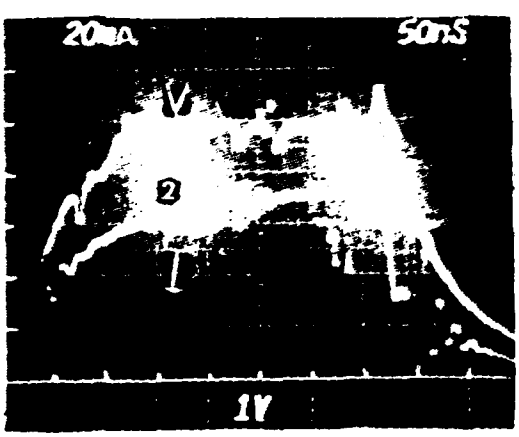

(e)

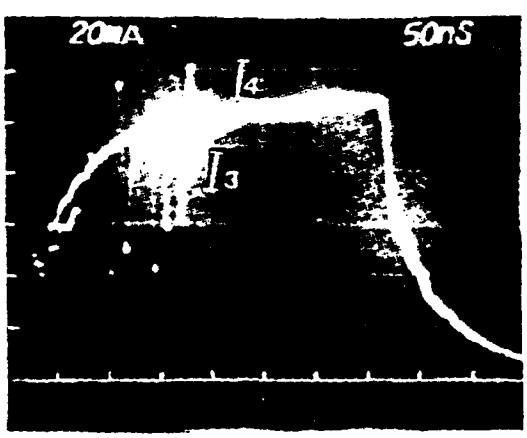

(f)

Figure 3.2.6

Comments: Comparison of the foregoing results with those for the two-contact technique in Figure 3.2.5(a) through (f), indicates strong differences. The current in the three-contact technique breaks into erratic oscillations at a low input voltage of only 3.5 V in Figure 3.2.6(a) and the amplitude of the oscillations is sufficiently high that a voltage source with low output impedance cannot hold the voltage steady; the input waveform in Figure 3.2.6(d) and (e) is changing erratically because of large variations of the load impedance.

Moreover, for the three-contact technique, a decrease in current as a function of time was not observed, and the transition to the low-conductance state occurred at lower voltages (data not shown here).

3.2.7 Triangular Pulse Response

Experimental procedure: The square-pulse generator (HP214), shown in Figure 3.1, was replaced by a Wavetek 155 generator to obtain triangular-shaped waveforms, and a diode was connected in series with its output to obtain pulses of single polarity. Sequences of triangular pulses were applied with varying amplitude and fixed duration. Selected responses are shown in Figures 3.2.7(a) through (d) as the pulse amplitude was increased

Figure 3.2.7 Triangular Pulse Response

Current waveforms as a function of time in response to triangular voltage pulses are shown in each figure. The negative-resistance-like behavior, hysteresis and oscillations [dotted part of current waveforms in Figures (c) through (f)], are observed as the voltage amplitude is increased above a certain threshold value.

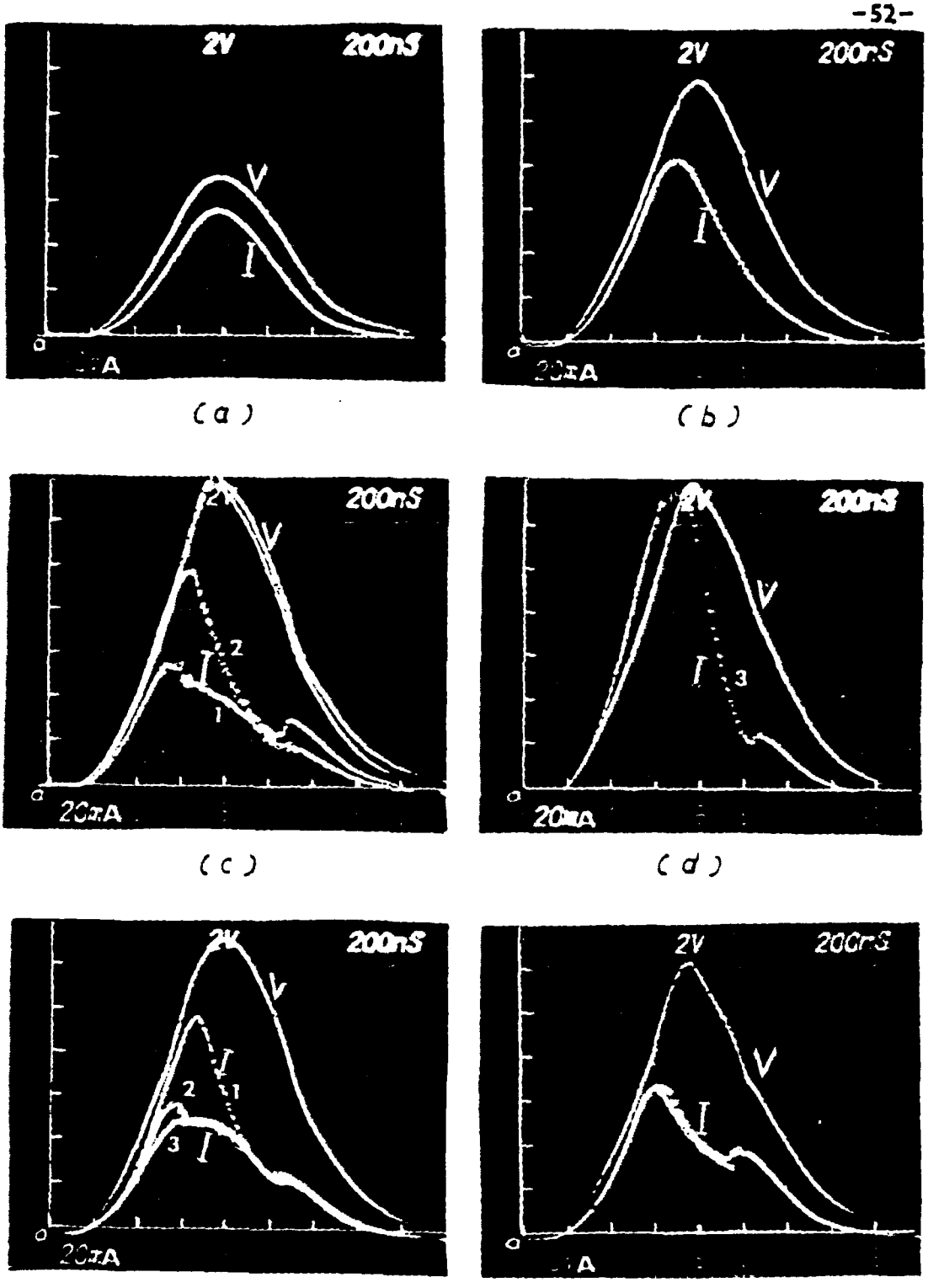

Figure 3.2.7

in small steps up to 14 V. Figures 3.2.7(e) and (f) show a few responses as the pulse amplitude is decreased. Responses upon repeated pulsing with unchanged input parameters are shown in Figures 3.2.7(c) and (d) for 14 V and similarly in Figure 3.2.7(e) for 13 V.

Comments: The triangular pulse response gives a composite view of all the different phenomena discussed earlier. As the voltage amplitude is increased above a certain value, the negative-resistance-like behavior, the hysteresis, and the oscillations appear. The dotted current waveform is due to the oscillations. Because the current decreases both as a function of voltage and as a function of time for fixed voltage, these responses show a complicated behavior.

Note the quantitative irreproducibility upon repeating the pulses at 14 V [Figure 3.2.7(c) and (d)] and at 13 V [Figure 3.2.7(e)].

3.2.8 Polarity Independence

The modified circuit, discussed in Section 3.2.7, was used without the diode in series to obtain alternate positive and negative triangular waveform.

Figure 3.2.8 shows a response of a single triangular wave. The negative-resistance-like phenomena, the hysteresis effect and the oscillations are observed during

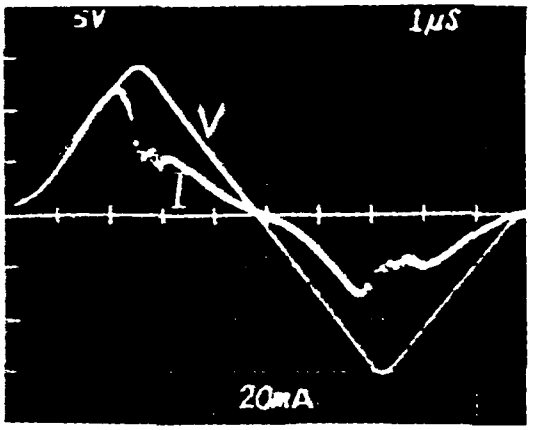

Figure 3.2.8 Triangular wave Response as a Function of Time

The current in response to a single triangular wave is shown. The input voltage is positive during the first half of the cycle and negative during the second half. All the phenomena observed during the positive half-cycle also appear during the negative half-cycle; during the latter half there is some phase delay caused by the changes that occurred during the first half-cycle.

both the positive and the negative half of the cycle. However, there is some phase delay in the negative half-cycle due to changes that occurred upon application of the voltage during the positive half-cycle.

3.2.9 Square-Pulse Response at Low Temperature

Experimental procedure: Figure 3.2.9(a) shows the response for an input pulse[15] of 4 V at room temperature. The temperature was then lowered slowly at a rate equal to or less than 5 K/min to 200 K using the Statham Test Chamber. At 200 K, sequences of pulses were applied with 200 ns duration and with amplitudes increasing in small steps. The current amplitude with the input pulse of 4 V was about 6 mA. The applied pulse of 15 V, and the current response is shown in Figure 3.2.9(b). Additional pulses were applied with increasing duration but fixed amplitude of 15 V. The input pulse with 600 ns duration and the current response are shown in Figure 3.2.9(c).

Figures 3.2.9(d) and (e) show the response upon repeated pulsing with amplitude and duration unchanged from the values shown in (c). Note the cumulative transition to the low-conductance state. The current drops from about 25 mA [Figure 3.2.9(c)] to a negligible value [Figure 3.2.9(e)]. The temperature was then increased very slowly to the room temperature value, and the room

Figure 3.2.9 Square-Pulse Response at 200 K in Time Domain

The reversible transition to the low-conductance state and the decrease in current with time during a single pulse are observed at 200 K.

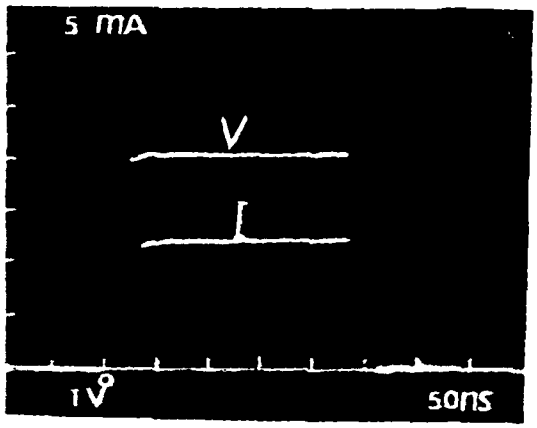

(a) R.T.

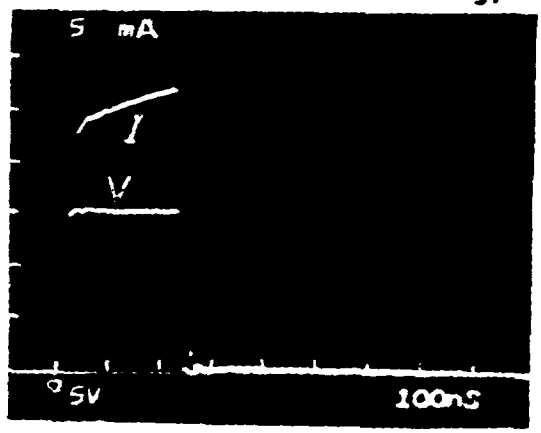

(b) 200 K

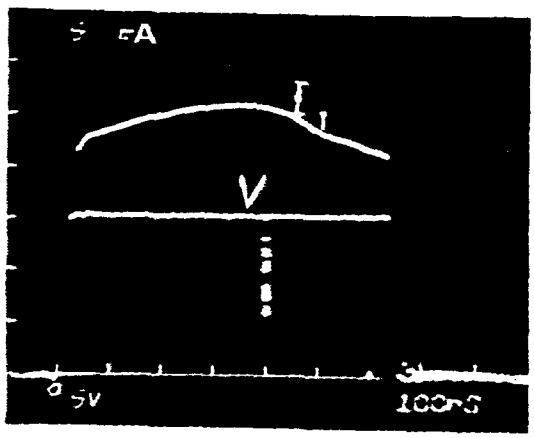

(c) 200 K

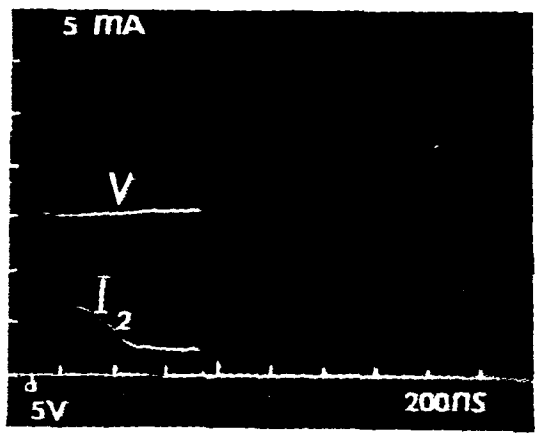

(d) 200 K

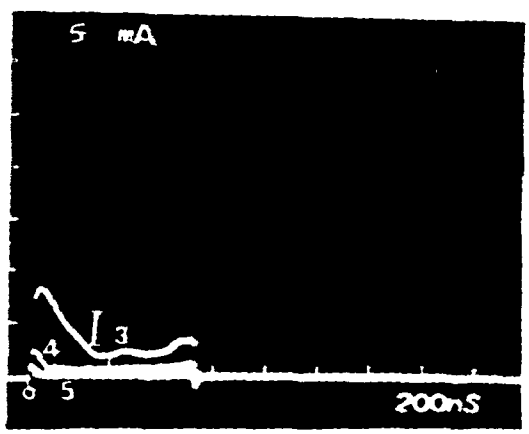

(e) 200 K

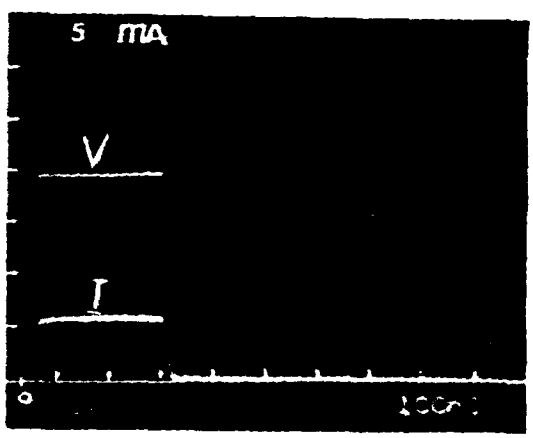

(f) R.T.

Figure 3.2.9

temperature response at 4 V is shown in Figure 3.2.9(f).

Comments: The experiment shows that the transition to the low-conductance state occurs even at 200 K. Upon warming, the sample recovers to some higher conductance state, but it is clear by comparison of Figures 3.2.9(a) and (f) that the sample conductance has not returned to the original value. Some other samples, during similar experiments, were found to recover at 200 K, just by application of pulses with decreasing amplitude (similarly to the cases at room temperature, in Section 3.2.1 and 3.2.5).

3.3 Discussion of the Results

3.3.1 Summary of the Phenomena

We have taken data on a large number of samples; in many cases the experiment has been performed more than once on the same sample. Only a representative fraction of the results has been described in Section 3.2, but the results on other samples were similar. The observed phenomena are summarized as follows:

(a) In general, it was observed that, as the voltage across the sample was increased from zero, the current initially increased. However, if the voltage was in-

creased above a certain value V_p, the current decreased with further increase in voltage. As the voltage was then decreased, the current increased again but with a large hysteresis effect.

This is not the full story. The value V_p at which the current peaks depends on the rate at which the applied voltage is varied. The negative-resistance-like behavior seems to appear at a somewhat lower voltage if the voltage is varied at a slower rate (see Figure 3.3.1). However, there was always some threshold. The decrease in current with increasing voltage is not a true static negative (differential) resistance, as evidenced by the variation of V_p and the large hysteresis effects; thus, we refer to it as the "negative-resistance-like" behavior.

(b) The second related phenomenon observed was that, if a voltage above a certain threshold value was applied at $t = 0$ and held constant, the current decreased with time after some delay time t_d. Most of the time, this phenomenon occurred even at voltages less than V_p. We cannot make any statement to compare the threshold voltage of this phenomenon with that of the negative-resistance-like phenomenon. The time t_d varied erratically upon repeated pulsing with fixed voltage.

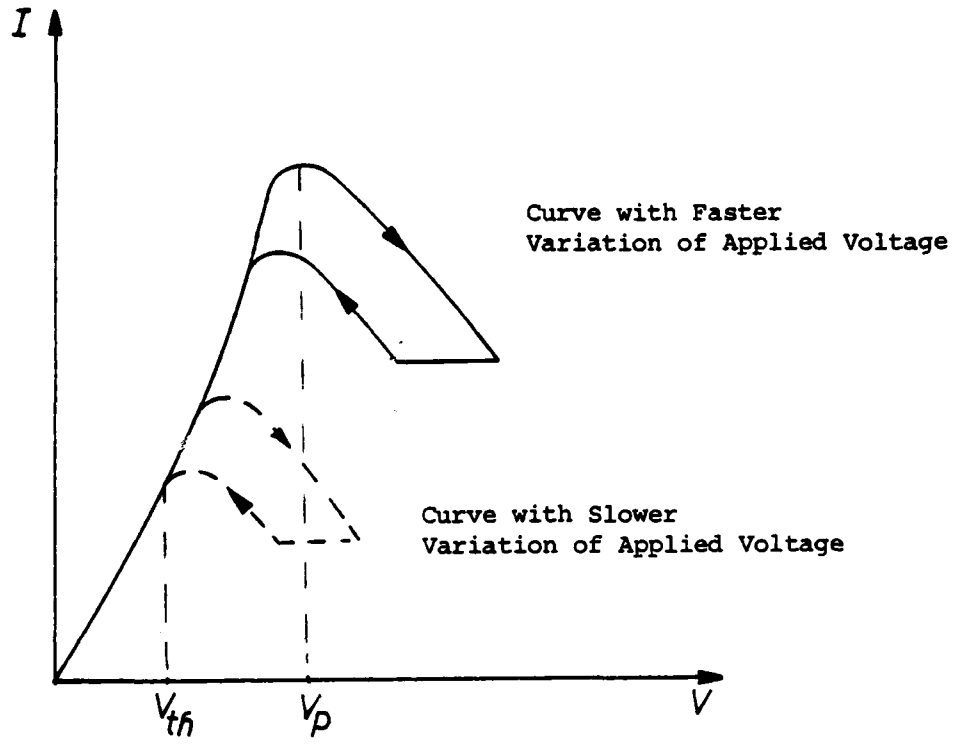

Figure 3.3.1 Phenomenological Relationship between Current and Voltage.

This is not a dc phenomenon. The relationship also depends on the rate at which the applied voltage is varied. The voltage V_p is that at which the current peaks. The voltage V_{th} is the threshold voltage required before the phenomenon is observed.

(c) Upon application of voltages much higher than the value at which the current peaks, there was a cumulative drop in the sample conductance. The drop in the conductance was either partly or completely reversible by one of the following processes: (1) by applying pulses of smaller amplitudes than the value at which the transition occurred, (2) by applying a voltage with opposite polarity, (3) by leaving the sample alone for a few seconds to several days.

(d) Often the current waveforms were superimposed with erratic oscillations. The oscillations turned on and off several times during a single pulse. The erratic occurrence of the oscillations with nonuniform amplitude made it impossible to measure the frequency accurately. For a large number of results from different samples, it was possible to read the approximate frequency from the waveform on the oscilloscope. In all such cases, the frequency was consistently found close to 70 MHz ± 10 MHz. One might think that the oscillations are due to circuit effect. However, upon variation of the frequency of a small ac test voltage, no resonance was observed.

(e) On a few samples the voltage pulse experiment was repeated at various temperatures ranging from 300 K to 200 K. All the phenomena that were observed for these

samples at 300 K also occurred at low temperatures. The negative-resistance-like behavior and the decrease in current with time during a single pulse were observed at temperatures down to 200 K (e.g., Figure 3.2.9). The oscillations have also been observed once at a temperature of 239 K. Voltage pulse experiments at low temperatures were only performed early in the course of this research and have not been studied extensively.

(f) The author is aware that the data have been presented with little quantitative detail and all the phenomena have been discussed only qualitatively. It was found impossible to study the phenomena in detail because of extremely poor quantitative reproducibility which was present even upon repeated experimentation on the same samples. All the efforts to achieve better reproducibility by improvement of the contacts and other experimental techniques and careful selection of the crystals with good morphological quality were unsuccessful. For example, evaporation of gold strips or utilization of the constant voltage source did not improve the reproducibility. It appears that a sample behaves differently upon repetition of experiments because there are actual changes going on within the sample under applied electric field. Some of these changes are not fully reversible upon the removal of the field. Similar erratic behavior

has also been reported by Warmack et al. for dc conductivity versus temperature and he also concludes that changes within the samples are the probable cause.[1]

3.3.2 Bulk or Interface Effects?

Attempts were made to determine if the changes in the sample conductance upon application of high-voltage pulses occurred uniformly in the bulk of the sample. On a few samples the dc bulk conductance was measured using the technique similar to the standard four-point probe method. The dc conductance was measured before and after performing the voltage pulse experiment. The contact configuration and the circuit shown in Figure 2.3.1 were used. The outermost contacts #1 and #4 were used for pulse experiments. The dc conductance was measured by passing a small dc current between contacts #1 and #4 using a constant-current source, and the potential drop V_{23} was measured between the two inner contacts using a high-input-impedance voltmeter. Power dissipation was kept much less than a microwatt. Data were taken with both positive and negative current and the linearity of the I-V relation was confirmed.

In general, the ratio I/V_{23} measured before and after the voltage pulse experiment was found different; however, the changes in conductance between contact 2 and

3 due to high-voltage pulses seemed to be very small. Most of the changes in the sample conductance took place at random either between contact 1 and 2 or between 3 and 4. The data suggest that the changes in the sample are localized, not uniform and that most of the changes occur either at the contact interface or in the bulk but close to the contacts. Conceptually, there is a vast difference between these two possibilities, but experimentally they are not easy to distinguish. Because of the importance of the distinction in explaining the physics behind the phenomena observed, a significant effort was made to determine whether the effects are at the contact interface or in the bulk. The question is not resolved with absolute certainty, but on balance the bulk effect appears to be the choice. The arguments against interface effects are as follows:

(a) The changes in conductance occurred randomly near either the positive or the negative electrode.

(b) All the phenomena discussed in Section 3.2 were observed regardless of the kinds of contacts, except when a silver paint contact was made on the sample (reasons discussed below).

(c) I-V relationships controlled by an interface effect (such as tunneling, Schottky barrier or chemical reaction effect) are normally unsymmetric with respect

to the polarity of the input voltage. As a matter of fact, silver paint makes a rectifying contact on the TTF-I_n crystal. Figure 3.3.2 shows typical I-V characterics with one of the two contacts made by applying silver paint on a bare sample (not over evaporated gold), and the other made with colloidal graphite. The result was taken with a sinusoidal wave source at 0.02 Hz. We believe the silver paint contact rectifies[17] because of the modulation of the AgI layer at the Ag and TTF-I_n interface[18]. We have shown in Section 3.2.8 that the negative-resistance-like behavior, the hysteresis and the oscillations appear during both the positive and the negative half cycles of a triangular wave input. If the observed phenomena occur near the same contact during both the positive and the negative voltage sweep, this observation would add weight to the plausibility argument for the bulk effect. Results of a different experiment, performed on several other samples, strongly suggests that the phenomena occur on the same contact. This experiment is as follows: High-voltage pulses of one polarity were applied to a sample until transition to the low-conductance state occurred. Then it was established that the change had occurred near a certain contact. After bringing the sample back to some higher conductance state, the foregoing procedure was repeated with voltage

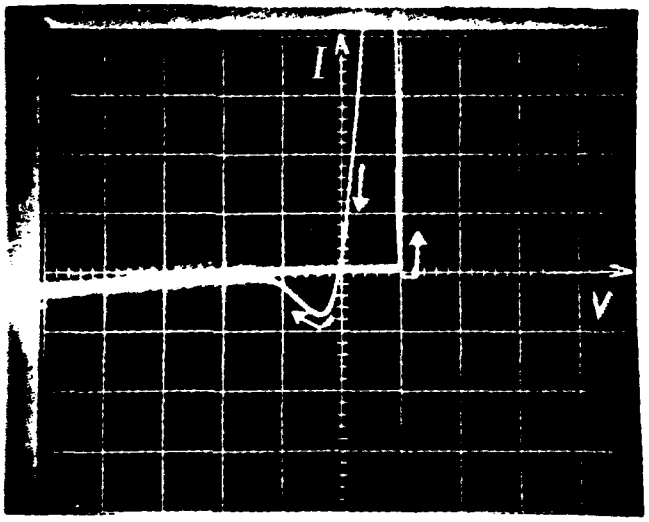

Figure 3.3.2 I-V Characteristic of the TTF-I_n with Silver Paint Contact as the Negative Electrode and Colloidal Graphite as the Positive Electrode.

The result was taken with sinusoidal wave source with 2.6 V amplitude, at 0.02 Hz. Due to chemical reaction between the sample and the silver, the characteristic is different for different polarities of input voltage. This is a single cycle display; repeated cycles exhibit considerable jitter.

pulses of opposite polarity. Most of the time, the change in conductance was found to be near the same contact.

(d) The experiments were performed with the contacts made on the side of a sample and also with the contacts made on the two ends as illustrated below.

The contact interface at the side and at the ends of the crystal, which has an anisotropic structure, should be quite different. However, all the phenomena were observed with both the end contact and the side contact.

The four foregoing arguments combined strongly suggest bulk effects. The effects are close to the contacts, possibly because the field and current density are likely to be higher near the contacts than away from them.

A note of caution: one should be careful before directly relating a change in the I/V_{23} ratio with a change in the bulk. In quasi-one-dimensional conductors the current throughout the cross section of the sample is not uniform. Localized changes in conductance could change the current through the group of filaments under investigation, even though the current through the exter-

nal circuit is kept constant. Moreover, one cannot completely rule out contact effects at either contact #2 or #3 because, even though they are open during the voltage pulse experiment, current could flow through the contacts as shown below.

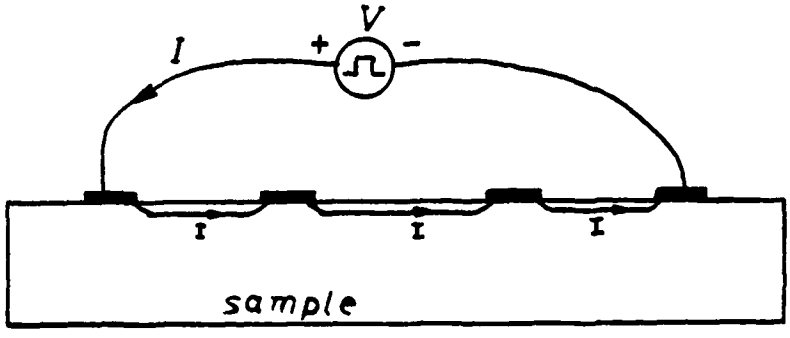

3.3.3 Calculation of Rise in Temperature due to Joule Heating

For end contacts, the current flows through the entire cross section of the crystal, and it is possible to estimate the energy density dissipated. When the current behaved abnormally, the dissipation was calculated for some of the samples and was found to be of the

order of 0.4 J/cm^3; and, in one case, it was found as low as 0.04 J/cm^3. The change in temperature ΔT can be estimated as follows:

$$\Delta T = (\text{energy/volume})/(\text{density} \times \text{specific heat})$$

The density of the material can be calculated by adding the mass of the elements per sublattice cell and dividing the number by its volume. The mass of a cell with four TTF molecules and approximately 2.8 iodine ions is approximately 20×10^{-22} g. Its volume is 9×10^{-22} cm^3. Thus, the density is about 2 g/cm^3. The specific heat of the crystal is unknown but if assumed to be about 4 J $g^{-1}K^{-1}$ ($\cong$1 Cal $g^{-1}K^{-1}$ = Specific Heat of Water) a dissipation of 0.04 J/cm^3 energy density would raise the temperature by less than 0.01 K. In the foregoing calculation of the energy density, it was assumed that the energy is dissipated uniformly throughout the sample. Even for end contacts, the potential drop is found to be higher near the contacts than away from them. Therefore, one cannot completely rule out localized heating effects.

4. MODEL

4.1 The Phenomenological Postulate of Two Distinct Conductivity States

The data suggest, and most data can be explained at least qualitatively by this assumption, that the material has two states with different conductivity (Figure 4.1). Initially, under zero field, the material is in the higher conductivity (HC) state and the current density increases with the field. However, as the field is increased to a critical value, the material switches into the lower conductivity (LC) state. As the field is reduced below the critical value, the material eventually returns to the HC state, but there is an appreciable delay, leading to a strong hysteresis effect. The critical value of the field is not sharply defined and increases with the rate at which the field is increased from zero. However, a certain threshold dc field is definitely required before the transition occurs. If the applied field is significantly higher than the critical value, the material stays, semipermanently, in the LC state even after the field is removed. In some cases, such a persistent change is caused by application of a lower field (but still above the threshold value) for long enough duration.

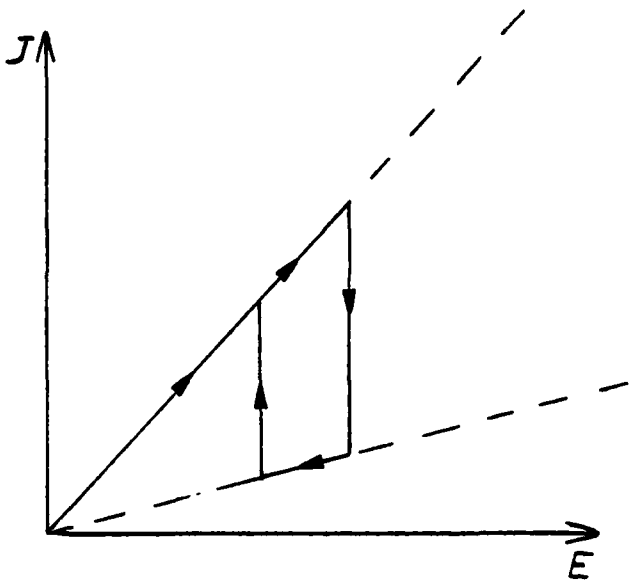

Figure 4.1 Phenomenological Relationship between Current Density and Electric Field for TTF-I_n ($n \cong 0.7$)

The material seems to swtich between two states, with a hysteresis effect, as the field is varied.

4.2 Field-Driven Transverse Disorder of the Iodine Sublattice

The following is an attempt to explain the mechanism that could be the cause of the abnormal electrical conductivity. The model is based on the basic facts about the structure of the ordered phase of TTF iodide as described in Section 1. The structure strongly suggests that, in the absence of imperfections and impurities, the iodine chains can freely slide along the smooth array of channels formed by the TTF sublattice.

However, in reality the samples will not be perfect crystals and structural defects and impurities are likely. Small amounts of disorder along the iodine chain due to formation of tri-iodide molecules are also possible.[5] In any event, the iodine chains in the crystal must be pinned at various points because of one or more irregularities. A finite segment of the iodine chain with pinned ends can be represented by a ball-and-spring model. This model consists of a one-dimensional stack of balls, connected to each other by nonlinear springs, sitting in a pipe of finite length with one or more balls immobile at each end. The compression of the springs

will be opposed by the force which is equivalent to the repelling Coulomb force between two iodine ions. The dilation of the spring will be opposed by the force which is equivalent to the electrostatic attraction between the positively charged TTF stacks and the negatively charged iodine stacks. As shown in Figure 4.2.1, if all the balls are forced to move in the same longitudinal direction, at one end the chain will be compressed and at the other end it will be dilated.

Even though the iodine-stack period and the TTF-stack period are not related, the iodine stacks themselves are phase locked with each other to form a monoclinic sublattice. The impurities and defects should be spread randomly throughout the crystal; thus, all the chains will not be pinned at the same points along their length. Accordingly, as soon as the iodine ions move, the transverse order, that is, the interchain order of the iodine sublattice, must get disrupted. The effect is illustrated in Figure 4.2.2. The solid lines represent the TTF columns and the circles represent the iodine ions. Pinned iodine ions are indicated by full circles. Under high field, the iodine chains will get deformed according to the ball-and-spring model. Transverse disorder can occur, for example, if the dilated end of one chain is next to the compressed end of another chain.

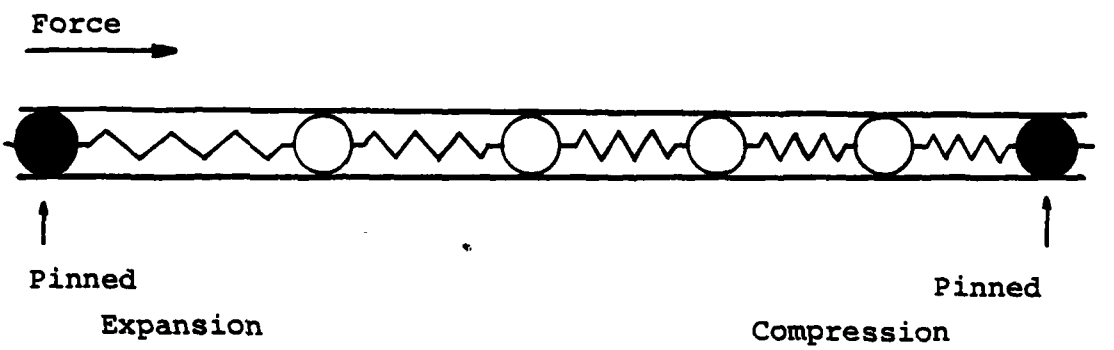

Figure 4.2.1 Ball-and Spring Model Representing Iodine Chain with Pinned Ions, Deformed due to External Force

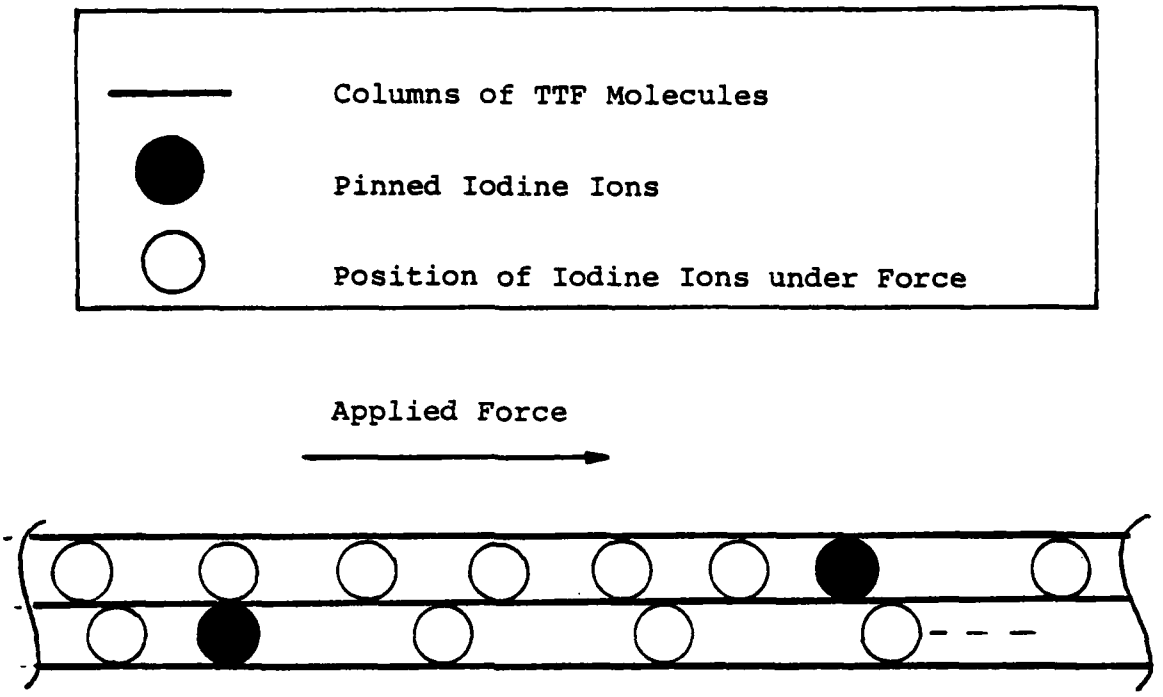

Figure 4.2.2 Disruption of the Transverse Order

The motion of iodine chains is likely to be restricted by random pinnings along their length. Accordingly, transverse disorder must occur.

The destruction of the transverse order follows directly from the postulate that the iodine ions are mobile along the channels formed by the TTF columns and that their motion is restrained by the impurities and defects in the crystal structure. As the iodine chains are deformed under high field, the transverse disorder must occur long before the changes in iodine concentration become significant. One might expect the destruction of the transverse order to affect the high longitudinal electronic conductivity of the ordered form of TTF iodide.

4.3 Transition to a Low-Conductivity Phase of Fully Disordered Iodine Sublattice

The exact connection of the transverse disorder and the electronic conductivity is not clear. We speculate that the interchain disorder further leads to intrachain disorder of the iodine ions. In other words, as soon as the iodine sublattice loses the transverse order, it "evaporates" and becomes fully disordered, while the TTF sublattice remains essentially unchanged.

The plausibility arguments for the foregoing speculation are based on the following background information: In the TTF halides, the ordered halide sublattice becomes

unstable at low concentration ($n < 0.7$).[5] Each TTF halide forms a stable disordered phase in which the halogen ions form a "gas-like" phase with random positions within the channels, while the TTF sublattice remains essentially the same.[5] For the TTF iodide system, a stable disordered phase exists at $n = 0.69$.[2,5] Figure 4.3 shows a likely qualitative relationship between the free energy and the composition parameter of the disordered and the ordered TTF halide system. The energy minima for the stable ordered phase and the stable disordered phase are labeled as A and D, respectively. It is conceivable that, under high field, the transverse disorder might trigger the transition from the ordered phase to the disordered phase, without any change in the composition.

Formation of a disordered phase seems to be the simplest and the most plausible mechanism which can explain large, semipermanent changes in conductivity. We have not been able to find any electronic conductivity data for the disordered-phase crystal that is stable at lower composition. However, if the iodine sublattice is disordered, with or without the composition shift, the

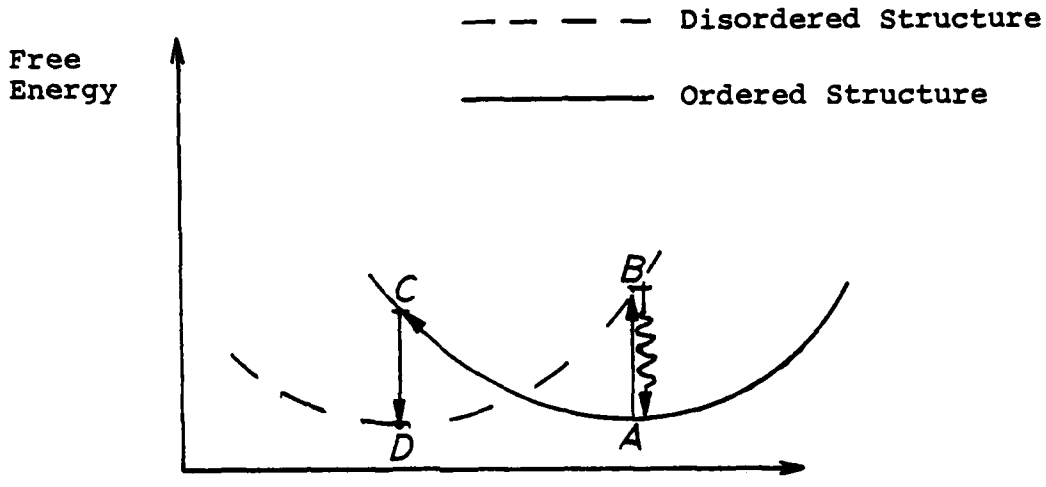

Figure 4.3 Qualitative Relationship of Free Energy and Composition Parameter n

A → B shows transition from the ordered phase to a "disordered phase" with fixed composition. A → C → D shows the transition to a disordered phase with composition shift to a lower n. A → B might conceivably be triggered by the disruption of the transverse order.

carriers (holes) along the TTF stacks might become localized rather than forming unlocalized mobile holes. In this event, the conductivity of the crystal in which the iodine ions are disordered should be appreciably lower than that of the fully ordered crystal.

Based on the foregoing speculation, it seems plausible that domains of disordered phase would form in parts of the TTF-I_n (n ~0.7) crystal that are under high field. In the case of quasi-one-dimensional conductors, in which the current perpendicular to the stacks is small, the formation of even a localized high resistivity region would directly affect the current along the entire length of the stack. This effect would occur even for the disordered region much shorter than the entire length of the stack.

Upon removal of the field, the reverse transiton to the ordered phase (B to A, in Figure 4.3) should occur because the composition would remain at that value for which the ordered phase is more stable. However, the reversal might take a fraction of a second to a few days. This would explain the recovery of some samples from the low-conductance state as a result of aging. Moreover, the transition from the disordered to the ordered phase might possibly be stimulated by "shaking" with voltage

pulses of smaller amplitudes or reversed-polarity voltage pulses.

4.4 Alternate Explanations: Effects of Changes in Local Iodine Concentration on the Electronic Conductivity

Significant deformation of iodine chains could also cause variations of the iodine concentration in the vicinity of the pinning points, as illustrated earlier by the ball-and-spring model. If the transverse disorder does not affect the intrachain order of the iodine sublattice, it is possible that enough modulation of local iodine concentration might occur to affect the electronic conductivity. There are at least two possible mechanisms through which the conductivity of the crystal might be affected:

(a) Formation of stable disordered phase ($n < 0.7$) in the vicinity of the pinning points due to iodine depletion.

As mentioned earlier, a stable disordered phase exists in the TTF iodide system at a composition parameter of $n \cong 0.69$. It is conceivable that, under applied field, depletion of iodine ions in the vicinity of the pinning points might lead to formation of local disordered phase. The transition might follow the path A→C→D, as

illustrated in Figure 4.3 If the disordered phase at D has a lower conductivity than the ordered phase at A, domains of disordered phase should lower the sample conductance in a similar manner as that discussed earlier for the disordered phase B.

Upon removal of the field, the elastic energy stored in the deformed iodine chains would change the crystal back to the ordered phase (A). It is possible that the reverse transition might occur as soon as the field is removed, or after a fraction of a second, or a few days. Therefore, formation and dissociation of disordered phase caused by changes in local iodine concentration is also a possible explanation for the semipermanent changes in sample conductance observed during the pulse experiment.

(b) Conductivity modulation due to changes in carrier concentration in a narrow energy band.

The hole concentration on the TTF stacks should be equal to the iodine concentration (Section 1.1.1). The electrical conductivity σ must depend on the iodine ion concentration. Normally, σ should be roughly proportional to $n(2-n)$, because the σ must be approximately zero both for no holes on the TTF stacks ($n = 0$) and for an empty TTF valence band ($n = 2$). According to the ball-and-spring model, there should be changes in iodine concentration in the vicinity of the pinning points, when

the chains get deformed. One might expect abnormal behavior in electronic conductivity of the crystal related to changes in local iodine concentration.

However, assuming no phase transition or molecule formation occurs, the deformation of the iodine chains will be limited by the size of the ions. The inter-iodine spacing at the compressed end must stay larger than the ionic diameter. The observed drop in conductivity, which is at least an order of magnitude under high pulsed field, can only be explained if the energy band is so narrow that the full band (no holes) condition can occur at an intermediate value of n. The nature of the ground state of this material is not yet established; thus, it is difficult to make any comment on the plausibility of the foregoing argument. However, as a result of weak residual forces between the TTF and the iodine ions, it is not inconceivable that for certain intermediate values of n, say n = 1, one finds Peierls-like insulating phases.[19] A Peierls instability is the cause of metal-to-insulator transitions at low temperature in several quasi-one-dimensional conductors.[20-22]

4.5 Attempts to Explain the Oscillations

The cause of the erratic oscillations with fixed, reproducible frequency, is not clear. If the oscillations were simply random noise bursts without any specific frequency they would readily fit, as fluctuations, into a model of ours which involves a phase transition. The mystery is the regular "frequency." The frequency is too high and the amplitude is too erratic for the oscillations to be the effect of parasitic components of the circuit. In any event, we have not found any such circuit resonance. One possible explanation follows from the disordered phase model used earlier to explain negative-resistance-like behavior. A material with bulk negative differential resistance is known to have travelling domains of high resistivity.[23] Annihilation of the domains at one of the electrodes and renucleation at some nucleating center might cause the current to oscillate.[23] Assuming that TTF-I_n ($n \cong 0.7$) has a true bulk negative differential resistance, one might think of travelling domains of disordered phase as the cause of the oscillations. However, it is difficult to explain the frequency that was found to be roughly 70 MHz for various samples, to be independent of the sample size or morphological quality, and irrespective of whether the contacts were

made on a side or at the ends. The domain of the disordered phase should not be able to travel faster than the speed of sound. Assuming the velocity is about 10^5cm/s, the length of the active region through which the disordered phase would travel should be about 0.0014 cm or 14 μm [$(10^5\text{cm/s})/(7\times10^7\text{Hz})$]. At this time, we have no idea what would constitute an active region of such a dimension and why the dimension would be the same for different samples of the crystal.

5. SUMMARY AND CONCLUSION

Abnormal behavior in the electronic conductivity has been observed for the ordered form of TTF-I_n ($n \cong 0.7$), under high pulsed bias. The anamolous behavior includes: (a) decrease in current with increasing voltage, (b) a reversible decrease with hysteresis, (c) slow semipermanent changes, (d) decrease in current as a function of time while the voltage is held constant, and (e) erratic occurrence of oscillations with the frequency of approximately 70 MHz.

Based on the structural properties, we postulate (a) that the crystal undergoes an electrically driven phase transition on the iodine sublattice and (b) that localization of charges along the TTF stacks is the explanation for the large changes in the electronic conductivity. The crystal structure strongly suggests that the iodines are mobile within their channels. The electric forces on the iodine ions are expected to cause modulation of iodine concentration in the vicinity of the pinning points. In addition to the intrachain order, there is also interchain order among the iodine chains. When the iodine ions move, the interchain order will be disrupted long before any significant changes in the local iodine concentration occurs. In other words, there are at least

two distinct consequences of the motion of iodine in such a restrained environment. In either event, the final result is that the iodine sublattice becomes disordered.

We were unable to study the current response quantitatively because, upon repeated experimentation, a given sample behaved differently. All indications are that under high field, localized changes that are erratically reversible occur within the sample. Such changes could be attributed to formation and dissociation of local disordered phases.

Not all the data can be explained using the field-driven disorder model. There are many questions still unanswered. The most puzzling one is the cause of the erratic occurrence of oscillations with, seemingly, a single frequency that is repetitive even from sample to sample.

To confirm the model presented here, more sophisticated experiments than just studying current response under pulsed bias would be required in conjunction with bigger and better-quality crystals. Specifically, the following experiments might be useful. (a) A study of the crystal structure under high pulsed fields. Most of the changes in the electronic conductivity have been found, randomly, near one of the electrodes because fields and current density are likely to be higher in

that region. One might be able to apply high fields closer to the middle of the sample by shaping it like a dumb-bell, as shown below.

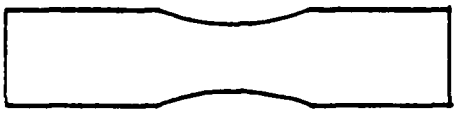

(b) Measurement of the electronic conductivity of the disordered phase ($n \cong 0.69$) of single-crystal TTF halides. (c) A direct experimental determination of ion mobility in the TTF halides should be performed. This is difficult because the high electronic conductivity would mask the ionic conductivity in most experiments. Materials with both high electronic and ionic conductivity are rare.[24]

References

1. R.J. Warmack, T.A. Callcott and C.R. Watson, "DC Conductivity of Tetrathiofulvalene bromide ($TTF\text{-}Br_n$) and $TTF\text{-}I_n$ Single Crystals," Phys. Rev. B, Vol. 12, No. 8, pp. 3336-3338, October 1975; R.J. Warmack and T.A. Callcott, dissertation submitted by R.J. Warmack, University of Tennessee, 1976 (unpublished).

2. R.B. Samoano, A. Gupta and V. Hadek, "The Electrical and Magnetic Properties of $(TTF)(I)_{0.71}$," J. Chem. Phys., Vol. 63, No. 11, pp. 4970-4976, December 1975.

3. J.J. Daly and F. Sanz, "Hepta (tetrathiafulvalene) Pentaiodide: the Projected Structure," Acta Cryst. Vol. B31, pp. 620-621, 1975.

4. C.K. Johnson and C.R. Watson, Jr., "Superstructure and Modulation Wave Analysis for the Unidimensional Conductor Hepta-(tetrathiafulvalene) Pentaiodide," J. Chem. Phys., Vol. 64, No. 6, pp. 2271-2286, March 1976.

5. B.A. Scott, S.J. La Placa, J.B. Torrance, B.D. Silverman and B. Weber, "The Crystal Chemistry of Organic Metals. Composition, Structure and Stability in the Tetrathiafulvalinium -Halide Systems," J.

Am. Chem. Soc., Vol. 99, No. 20, pp. 6631-6639, September 1977.

6. S.J. La Placa, P.W.R. Cornfield, R. Thomas and B.A. Scott, "Non-Integral Charge Transfer in an Organic Metal: The Structure and Stability," Solid State Communications, Vol. 17, No. 5, pp. 635-638, 1975.

7. For TTF-I_n, the range in composition of $0.71 \leq n \leq 0.77$ has been observed by Samoano et al. [ref. 2], while La Placa et al. [ref. 6] and Scott et al. [ref. 5] have reported $0.72 \leq n \leq 0.74$ and $0.7 \leq n \leq 0.72$, respectively.

8. G. Theodorou, "Lattice Distortions in Tetrathiofulvalinium Bromide [$(TTF)Br_{0.74-0.79}$]," Phys. Rev. B, Vol. 19, No. 2, pp. 1132-1135, January 1979.

9. J.B. Torrance and B.D. Silverman, "Charge Transfer and Ionic Bonding in Organic Solids with Segregated Stacks," Phys. Rev. B, Vol. 15, No. 2, pp. 788-801, January 1977.

10. See, for example, C.W. Keenan and J.H. Wood, General College Chemistry, Harper and Row, New York, 1966, p. 216.

11. Acheson's Micrographite in aqueous base (Aquadag®).

12. Dupont #4817.

    Silver paint contacts made directly on the sample rectify. The same contacts have been described as "poor" or "insulating" by other groups [see ref. 1,2].

13. Model LT-3-110, Air Products and Chemicals, Inc., Allentown, PA. The temperature is controlled with a combination of liquid nitrogen and an electric heater.

14. Model SD 60, Statham Instruments, Inc., Oxnard, Ca. It uses a closed air flow system to transfer heat to or from objects under test. An electric coil heater is used to heat the chamber. Cooling of the chamber is accomplished by injecting compressed CO_2 into the test chamber where the coolant rapidly evaporates.

15. The CEF circuit was not used, the pulses were applied directly from the pulse generator.

16. The scales specified with all the figures in Section 3.2 represent units/div; e.g, the scales for Figure 3.2.1(a) are 2 V/div and 50 mA/div.

17. Within the applied voltage range the colloidal graphite makes ohmic contact.

18. Such a reaction was already invoked by Warmack et al. [ref. 2] to explain the poor contacts made by silver paint to the TTF halides.

AD-A084 136 CALIFORNIA UNIV SANTA BARBARA F/G 7/4
THE ROLE OF IODINE MOTION ON THE ELECTRONIC PROPERTIES OF TETRA--ETC(U)
MAR 80 S M LATIF N00014-76-C-1044
UNCLASSIFIED NL

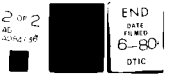

19. R.E. Peierls, Quantum Theory of Solids, p. 108, Clarendon, Oxford, 1975.

20. J.R. Fletcher and G.A. Toombs, "An Interpretation of the $2k_F$ and $4k_F$ X-Ray Scattering for Tetrathiafulvalene Tetracyanoquinodimethane (TTF-TCNQ)," Solid State Communications, Vol. 22, No. 9, pp. 555-556, 1977.

21. T. Sambougi, K. Tsutsumi, Y. Shiozaki, M. Yamamoto, K. Yamaya and Y. Abe, "Peierls Transition in TaS_3," Solid State Communications, Vol. 22, No. 12, pp. 729-731, 1977.

22. A. Kobayaski, Y. Sasaki, I. Shirotani and H. Kobayashi, "Evidence for a Peierls-Fröloch State of One-Dimensional Platinum Complex $K_{1.81}Pt(C_2O_4)_2-H_2O$," Solid State Communication, Vol. 26, No. 10, pp. 653-656, June 1978.

23. See, for example, B.K. Ridley, "Specific Negative Resistance in Solids," Proc. Phys. Soc. (London), Vol. 82, Part 6, No. 530, pp. 954-966, December 1963.

24. J. Kennedy, M. Kleitz (Chemistry Department, University of California, Santa Barbara), personal communication.